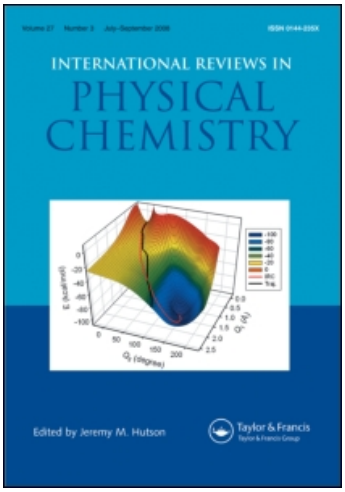

International Reviews in Physical Chemistry
Publication details, including instructions for authors and subscription information:
http://www.informaworld.com/smpp/title~content=t713724383

Vibrational spectroscopy of small-sized hydrogen-bonded clusters and their ions

Takayuki Ebata; Asuka Fujii; Naohiko Mikami

Online publication date: 26 November 2010

To cite this Article Ebata, Takayuki , Fujii, Asuka and Mikami, Naohiko(1998) 'Vibrational spectroscopy of small-sized hydrogen-bonded clusters and their ions', International Reviews in Physical Chemistry, 17: 3, 331 — 361
To link to this Article: DOI: 10.1080/014423598230081
URL: http://dx.doi.org/10.1080/014423598230081

INTERNATIONAL REVIEWS IN PHYSICAL CHEMISTRY, 1998, VOL. 17, NO. 3, 331–361

Vibrational spectroscopy of small-sized hydrogen-bonded clusters and their ions

by TAKAYUKI EBATA, ASUKA FUJII and NAOHIKO MIKAMI

Department of Chemistry, Graduate School of Science, Tohoku University, Sendai 980-8578, Japan

Vibrational spectroscopies of small-sized hydrogen-bonded clusters of organic acids and related molecules, as well as their ions, are reviewed based on our recent results. OH stretching vibrations of the jet-cooled clusters generated by supersonic expansions are observed by the various size-selected and population-labelling spectroscopic methods; ionization detected infrared (IR) and/or stimulated Raman spectroscopies for the neutral clusters in the electronical ground state (S_0) and fluorescence detected IR spectroscopy for the clusters in the electronically excited state (S_1). The hydrogen-bond structures of phenol-$(H_2O)_n$ clusters are extensively investigated on the basis of the spectral analysis combined with *ab initio* calculations of their stable forms and vibrations. Remarkable enhancement of the hydrogen-bond strength upon electronic excitation is demonstrated for the IR spectra of the S_1 clusters of phenol. For tropolone-$(H_2O)_n$ and $-(CH_3OH)_n$ clusters, $(phenol)_3$, and fluorobenzene-$(CH_3OH)_n$ clusters, cluster-size-dependent rearrangements and transformations of their hydrogen bonds are also investigated. IR dissociation spectroscopy of the cluster ions involving an ion-trapping technique is also described. The method is used to obtain vibrational spectra of $(phenol)_n^+$, $[phenol\text{-}(H_2O)_n]^+$ and $(phenol\text{-}benzene)^+$; their characteristic spectra of the OH stretching vibrations indicate that extremely large changes of the intermolecular hydrogen bonds are induced upon ionization of the clusters. Finally, a novel method for vibrational spectroscopy of bare molecular ions, for which no dissociation spectroscopic technique is successful, is described and its application to the IR spectrum of the phenol cation is given. The method involves autoionization process following vibrational excitation of the high-Rydberg-state molecule whose core has essentially the same vibrational structure as that of the bare ion. Future applications and directions of vibrational spectroscopy of clusters are discussed.

1. Introduction

Molecular-scale explanations of physicochemical properties encountered in macroscopic systems are a fascinating outcome of spectroscopic studies of molecular systems. Extensive development of supersonic molecular beam techniques allows us to study size-selected gas-phase molecular clusters, providing a medium for the microscopic investigation of the properties in bulk systems. Clusters in which a molecule is surrounded by other molecules are thought to be molecular-level models of solute–solvent systems. For example, solvent effects in bulk systems can be investigated on the basis of the stepwise clustering of solvent molecules. Despite the large distance in properties between the cluster systems and the condensed phases, one expects that collective chemical properties in solutions can be interpreted in terms of local structures and dynamics of the intermolecular surroundings. Spectroscopic investigations contribute substantially to the analyses of the intermolecular structures as well as their dynamical behaviour.

Among various systems, molecular clusters bound together by one or more hydrogen-bonds (H-bonds) are of special importance, because the binding nature is

0144–235X/98 $12.00

inherently related to many chemical properties, such as, acidity, basicity, proton (or hydrogen atom) transfer, and so on. Systems involving water clusters are of special interest in respect of the properties of aqueous solutions as well as in biological environments. Detailed information about intermolecular binding structures in those clusters provides substantial fundamental data for a microscopic view reflecting H-bonding networks in condensed phases. Recent progress of vibrational spectroscopies of size-selected gas-phase clusters has opened an appropriate way to characterize their intermolecular H-bond structures, providing direct information about the bonding sites.

Size-selected vibrational spectroscopy was first applied to cluster cations, since the size separability of clusters can readily be obtained with mass spectrometric methods. Well-known studies done by Lee and co-workers [1] demonstrated that the spectroscopy in the OH stretching frequency region is inherently effective to characterize the intermolecular structure of H-bonded clusters, such as hydrated hydronium ions. Extensive studies on various H-bonded cluster ions have been reported with the infrared (IR) photodissociation spectroscopy, as will be described in section 3.

For neutral clusters, on the other hand, the mass spectrometric method is not effective for size selection, thus vibrational spectroscopic studies of their neutral state(s) have appeared much later than those of ionic clusters. Huisken and co-workers [2] first reported an IR photodissociation spectroscopic study of small-size water clusters by using a novel size-selection technique involving molecular beam scattering which was developed by Buck and Meyer [3]. The direct high resolution IR absorption spectroscopic measurements for the water clusters has been extensively studied by Saykally and co-workers [4].

Recent progress of laser double resonance techniques leading to various kinds of population labelling spectroscopies has enabled us to obtain more detailed vibrational spectra of size-selected neutral clusters; electronic transitions are used for size selection as well as the extremely sensitive detection for the population change induced by vibrational excitations. A double resonant technique between stimulated Raman pumping for the vibrational excitation and a probe of the population by a UV laser was first applied by Owyoung and co-workers for gas phase NO and benzene [5], and the spectroscopy was extended to the clusters involving aromatic molecules by Felker and co-workers [6]. Double resonance spectroscopy between a tunable IR laser and a UV probe laser was first applied to benzene and benzene dimer by Lee and co-workers [7]. Size-selected IR spectroscopy was extended to the observation of CO stretching vibration by Brutschy and co-workers [8], and OH stretching vibration by our group [9] and by Zwier and co-workers [10, 11]. Since the nonlinear optical processes, such as optical parametric oscillation (OPO) and difference frequency generation (DFG) have become more widely used, IR spectroscopic studies on various H-bonded systems have been reported by many groups. It has been demonstrated that characteristic IR spectra of those systems are of substantial use for analyses of their intermolecular binding structures by using spectral simulations based on theoretical calculations with *ab initio* molecular orbital methods. An intensive review article describing H-bonding cluster systems has recently been given by Zwier [11]. In this paper, we will describe our results on vibrational spectroscopic studies of H-bonded clusters of organic acids and related compounds as well as those ions, representing an emphasis on the characterization of their intermolecular structures and dynamics. First, we discuss the neutral clusters of phenol, tropolone and fluorobenzene describing the size-selective spec-

troscopic methods for neutral clusters. Secondly, the spectroscopy of ionic clusters will be given together with novel spectroscopic methods for molecular ions and for cluster ions.

2. Neutral clusters

2.1. *Excitation scheme and experimental set-up*

Figure 1 (*a*) and 1 (*b*) shows excitation schemes of IR–UV and stimulated Raman-UV double resonance spectroscopies for clusters in the electronic ground state. The jet-cooled molecules or clusters are pumped to a specific vibrational level by tunable IR laser excitation (ν_{IR}) or by stimulated Raman excitation with pump and stokes lasers (ν_1, ν_2). The vibrational excitation leads to the depletion of the $v = 0$ level, which can be monitored by the electronic transition with the UV laser (ν_{UV}). The frequencies of the UV laser are tuned to vibronic bands of the S_1–S_0 transition, usually the 0,0 bands, of each species, so that the population probe of a particular species can be achieved. Either fluorescence or resonantly enhanced multiphoton ionization (REMPI) signal is monitored, and the population depletion induced by the IR or Raman pumping appears as reductions of their intensities. Thus, by scanning the tunable IR frequency ($h\nu_{IR}$) or the difference frequency ($h(\nu_1-\nu_2)$) of Raman pumping lasers while monitoring either fluorescence or REMPI signal, the fluorescence-dip or ion-dip vibrational spectrum is obtained. These spectroscopies can be called ionization (fluorescence) detected infrared spectroscopy, IDIRS (FDIRS), and ionization (fluorescence) detected stimulated Raman spectroscopy, IDSRS (FDSRS) [6].

Figure 2 (*a*) shows the set-up of IDIRS. The clusters were generated by a supersonic expansion of a gaseous mixture of solute/solvent diluted with He. The solute molecules were kept in a sample housing whose temperature was controlled to obtain enough vapour pressure. The mixture was expanded into vacuum through a pulsed nozzle having a 800 μm orifice. The IR and UV laser beams were focused into a vacuum chamber in a counterpropagated geometry. The tunable IR laser light was generated by difference frequency generation between the second harmonic of a Nd:YAG laser (70 mJ) and a Nd:YAG laser pumped dye laser (10 mJ) using a $LiNbO_3$ crystal, and its typical power at 2.7 μm is 0.5 mJ. The UV laser light was a second harmonic of a XeCl excimer laser pumped dye laser and its typical output power was 50 μJ. The vacuum chamber consisted of a main chamber and a sub-chamber. The former was pumped by a 6 inch diffusion pump and the latter was pumped by a 60 l s^{-1} turbo-molecular pump. The ions generated by REMPI were introduced to the sub-chamber by an ion-lens and either the total ions or mass separated ions with use of a time-of-flight tube were detected by an electron multiplier. The ion-current was amplified and processed by a boxcar integrator which was controlled by a personal computer.

Figure 2 (*b*) shows the set-up for FDSRS. A second harmonic of the Nd:YAG laser and the Nd:YAG laser pumped dye laser were used for the pumping and Stokes laser lights, respectively. The two laser beams were combined by a beam combiner and focused onto the supersonic free jet at 15 mm downstream with the counterpropagated geometry with respect to the UV laser beam. In the case of the fluorescence-dip measurement, the fluorescence was detected by a photomultiplier tube after passing through a band pass filter and the photocurrent was processed with the same boxcar integrator/personal computer acquisition system.

Figure 1 (*c*) shows the excitation scheme for IR spectroscopy to observe vibrational levels in the electronically excited state (S_1) [12, 13]. In this method, a particular cluster was excited to the vibronic level in the S_1 state, normally to the zero-point level, with

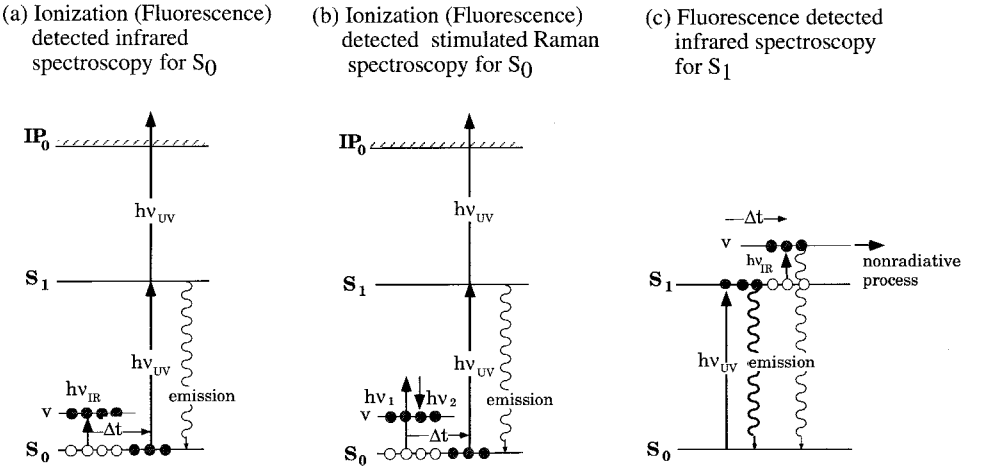

Figure 1. Excitation scheme of double resonance spectroscopy for the measurements of the vibrational levels of neutral species.

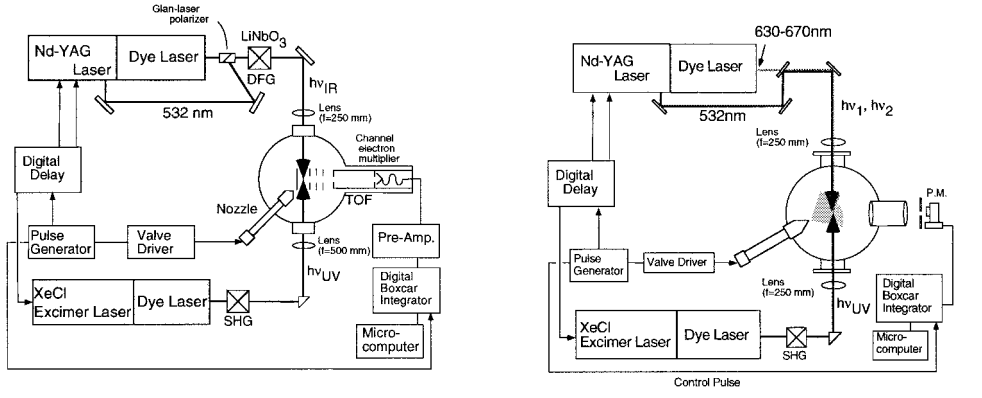

Figure 2. Experimental set-ups of (*a*) ionization detected infrared spectroscopy (IDIRS), and (*b*) fluorescence detected stimulated Raman spectroscopy (FDSRS).

the UV laser light, and its fluorescence intensity, which is proportional to the population of the cluster in S_1, was monitored. In this case, the IR pulse is introduced just after the UV laser pulse; a typical delay time was 5 ns. If the IR pumping rate to the vibronic level of S_1 is larger than the fluorescence decay rate and the fluorescence quantum yield of the level is lower than that of the zero-point level, the total fluorescence intensity decreases when $h\nu_{IR}$ is resonant with the vibrational transition in S_1. The fluorescence-dip spectra of the S_1 clusters are, thus, obtained by scanning $h\nu_{IR}$ while monitoring the total fluorescence. This spectroscopy is essentially FDIRS except that the delay time between the IR and UV pulses is opposite to that used for the observation of vibrational levels in S_0.

2.2. *Phenol-$(H_2O)_n$ in the S_0 state*

Phenol is a fundamental aromatic alcohol and its hydrogen(H)-bonded clusters with water or other protic molecules have been extensively studied by various electronic spectroscopies combined with supersonic jets [14–18]. Figure 3 shows the S_1–S_0 (1+1) REMPI spectra of phenol-$(H_2O)_n$ in the band origin region. Prominent

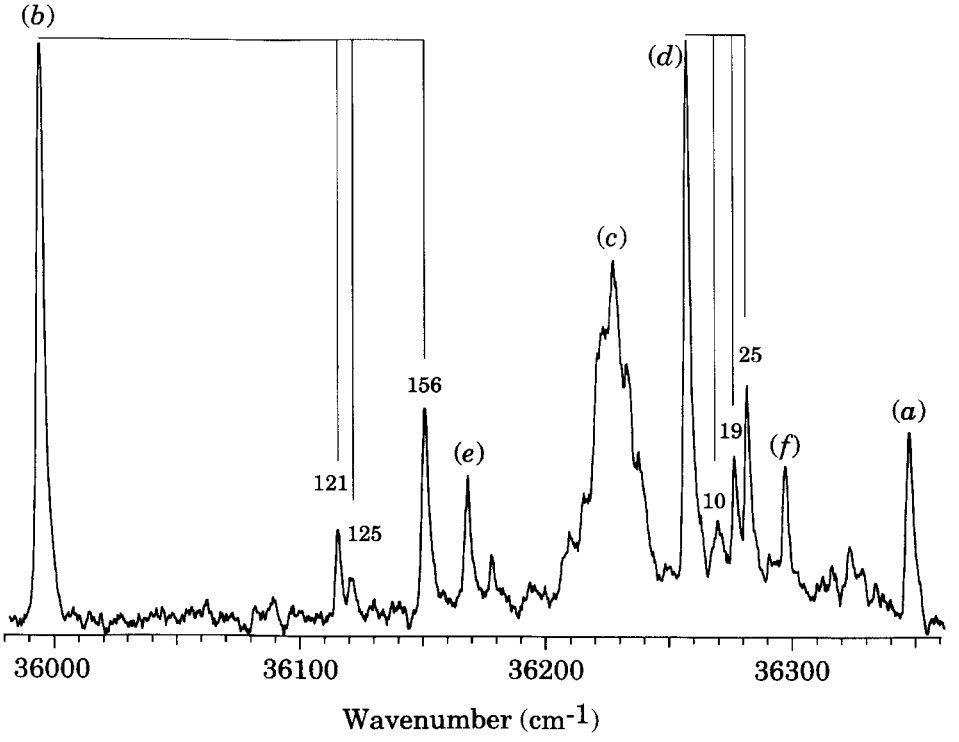

Figure 3. S_1–S_0 (1+1) REMPI spectrum of jet-cooled phenol and phenol-$(H_2O)_{n=1-5}$ clusters, showing the band origin region. The spectrum was obtained by detecting total ion current. (*a*) Bare phenol, (*b*) phenol-(H_2O), (*c*) phenol-$(H_2O)_2$, (*d*) phenol-$(H_2O)_3$, (*e*) phenol-$(H_2O)_4$ and (*f*) phenol-$(H_2O)_5$.

bands have already been assigned by several groups with REMPI-mass spectroscopic studies [15, 17, 18]. Among the various bands, the band (e) was first assigned to the 0,0 band of phenol-$(H_2O)_4$ and the band (f) to the 0,0 band of its isomer by REMPI-mass spectrometric study [18]. However, as will be described later, the obtained IR spectrum suggests that band (e) belongs to phenol-$(H_2O)_4$ and the band (f) belongs to phenol-$(H_2O)_5$.

2.2.1. *IR and Raman spectra of phenol and phenol-H_2O*

Figure 4 shows the IDIR and IDSR spectra of bare phenol and phenol-$(H_2O)_n$, $n = 1$–5 [9]. For bare phenol, both the IR and Raman spectra show the OH stretching vibration (ν_{OH}) at 3657 cm^{-1}. In the CH stretching region (ν_{CH}), on the other hand, a clear intensity alternation between the IR and the Raman spectra is seen for the totally symmetric ν_{CH} (3075 cm^{-1}) and asymmetric ν_{CH} vibrational bands.

For phenol-H_2O (figure 4(*b*)), two intense ν_{OH} vibrations are observed at 3524 and 3748 cm^{-1}. The former band is assigned to the OH stretching vibration of the phenol site. The frequency is reduced by 133 cm^{-1} from that of bare phenol, indicating that the OH bond strength is drastically weakened by the H-bond formation. The latter band is assigned to the antisymmetric stretching band (ν_3) of the H_2O site. The symmetric vibration (ν_1) of H_2O, on the other hand, appears at 3650 cm^{-1} in the Raman spectrum. This intensity alternation is similar to that of the bare H_2O molecule. In addition, the frequency shift of the two vibrations from bare H_2O (-7 cm^{-1} for ν_1 and -8 cm^{-1} for

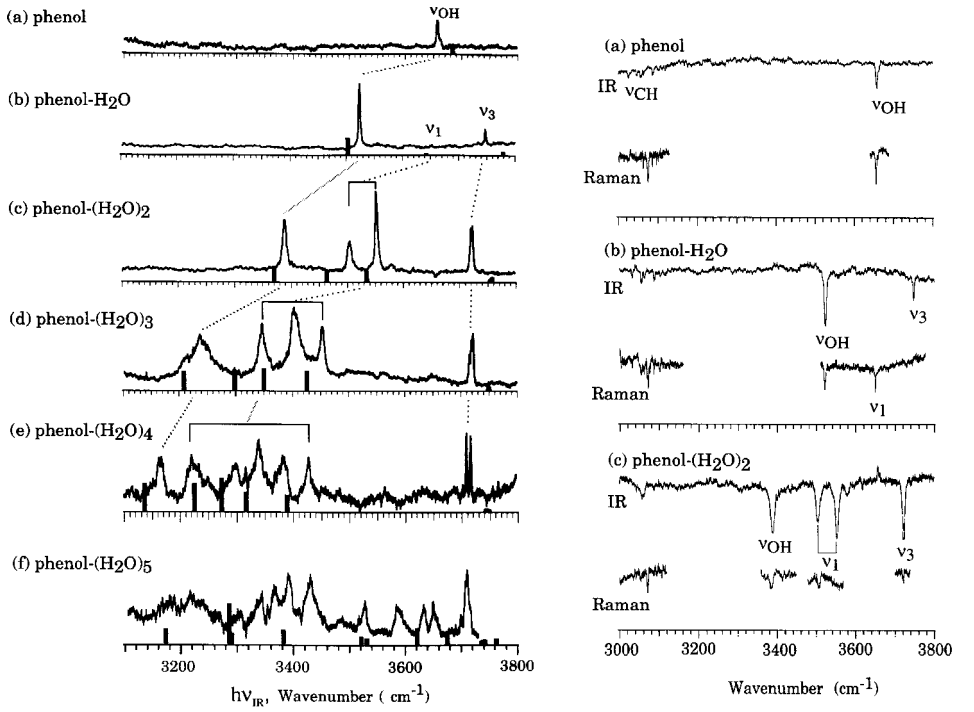

Figure 4. (left) IDIRS spectra of phenol and phenol-$(H_2O)_{n=1-5}$ clusters. The spectra are modified so that the band intensities are proportional to the absorption cross section [9]. The stick diagram is the absorption spectra obtained by the *ab initio* calculation with HF-SCF/6-31G* level [18]. (right) Comparison between IDIRS and IDSRS spectra of phenol and phenol-$(H_2O)_{n=1-2}$ clusters.

ν_3) is much smaller than phenolic OH stretch. Figure 5(*a*) shows the structure of phenol-H_2O obtained by an *ab initio* calculation performed by Watanabe and Iwata [19]. The structure is such that phenol acts as a proton donor and H_2O acts as an acceptor. A good agreement is obtained for the vibrational frequencies and intensities between the observed spectrum and calculated ones (stick diagram).

2.2.2. *Ring form phenol-*$(H_2O)_{n=2-4}$

Figure 4(*c*) shows the IDIRS and IDSRS spectra of phenol-$(H_2O)_2$. Five bands are observed in the ν_{OH} vibrational region; three bands at 3388, 3505, and 3553 cm^{-1} with broad bandwidths and two closely separated sharp bands at 3722 and 3725 cm^{-1}. The number of the observed ν_{OH} bands is equal to the number of OH oscillators of this cluster. The most stable structure obtained by *ab initio* calculation is the ring form as shown in figure 5(*b*), and the band structure is characteristic to the ring form cluster. In the ring form cluster, there are three H-bonded OH groups and two OH groups protruding from the ring. Therefore, as a first approximation, three bands at 3388, 3505 and 3553 cm^{-1} can be assigned to the H-bonded ν_{OH} vibrations in the ring and the bands at 3722 and 3725 cm^{-1} can be assigned to ν_{OH} free from H-bonds. According to the *ab initio* calculations, the lowest frequency band at 3388 cm^{-1}, is assigned to the H-bonded phenolic ν_{OH} and the other two bands are assigned to vibrational modes involving the symmetric OH stretching vibrations (ν_1) of H_2O sites. On the other hand, the bands that appear at 3722 and 3725 cm^{-1} are assigned to those involving the asymmetric OH stretching vibrations (ν_3) of the H_2O sites.

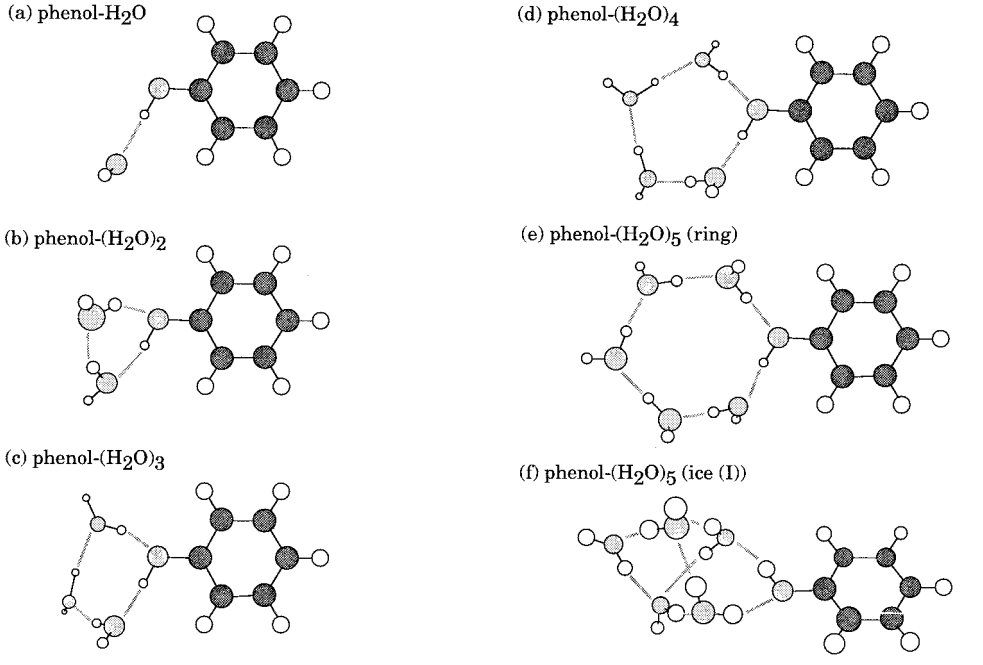

Figure 5. Structures of the stable phenol-$(H_2O)_{n=1-5}$ clusters. The structures were obtained by *ab initio* calculation with HF-SCF/6-31G* level [18].

As described above, the vibrational spectra of the ring form clusters have characteristic features, that is the H-bonded ν_{OH} vibrations become broad and shift to red, while the ν_{OH} vibrations free from the ring remain at $\sim 3720\ cm^{-1}$. The IDIR spectra of ring form phenol-$(H_2O)_3$ (figure 4(*d*)) and phenol-$(H_2O)_4$ (figure 4(*e*)) show similar spectral features, and the simulated spectra of the ring from clusters obtained by *ab initio* calculation (stick diagram) agree very well with the observed ones. For phenol-$(H_2O)_3$, the four bands at the lower frequency side are due to the ν_{OH} vibrations in the ring, and the three sharp bands at $\sim 3720\ cm^{-1}$ to the ν_{OH} vibrations protruding from the ring. According to the calculated results, the lowest frequency vibration consists mainly of H-bonded ν_{OH} of the phenol site, and the other three low frequency vibrations are attributed predominantly to the ν_1 vibrations of H_2O sites. The interval between the H-bonded ν_{OH} vibrations and those of ν_{OH} free from the H-bond increases with the cluster size and no band appears in this region, which we call a *window* region.

2.2.3. *Ice form phenol-$(H_2O)_5$*

The IDIRS spectrum of figure 4(*f*) obtained by monitoring band (f) at $36295\ cm^{-1}$ in figure 3, shows an anomalous spectral pattern. More than 11 ν_{OH} bands are seen and the cluster may be assigned to phenol-$(H_2O)_5$ or a larger cluster. Four ν_{OH} bands appear in the window region, indicating a structure different from the ring form. Watanabe and Iwata investigated possible isomers of this cluster, and suggested the most possible structure to be the 'ice-(I)' form, shown in figure 5(*f*) [18]. The ice-(I) isomer has almost the same stabilization energy with the ring form isomer (figure 5(*e*)), and has a solid-like structure different from the planer form ring clusters. The characteristic point of 'ice-(I)' is that two H_2O molecules in the cluster act as a double proton donor and the four bands appeared in the energy region 3500–3700 cm^{-1} are

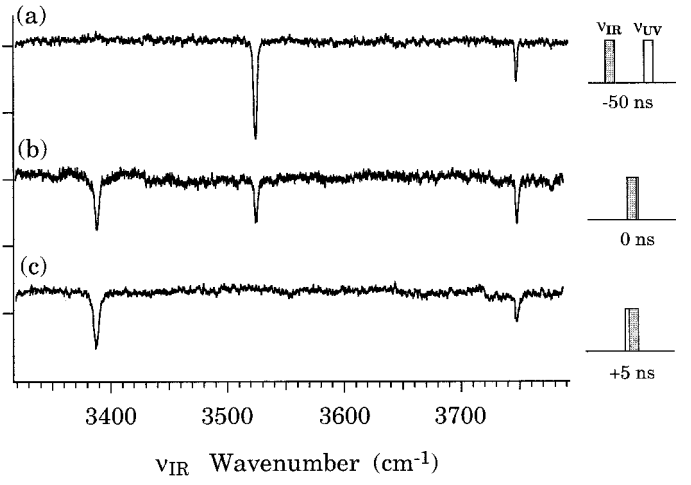

Figure 6. FDIRS spectra of phenol-H_2O measured at three different delay time. (*a*) The IR pulse is introduced at 50 ns prior the UV pulse. (*b*) The IR pulse is introduced with no delay with respect to the UV pulse. (*c*) The IR pulse is introduced at 50 ns after the UV pulse.

assigned to their ν_{OH} vibrations. Very recently, we also observed a similar vibrational structure in the IR spectrum of the 2-naphthol-$(H_2O)_5$ cluster, and the results suggest a similar change of the stable structure from the ring form to the ice form in the higher size clusters [20].

This ice (I) structure is also observed in the $(H_2O)_6$ clusters by Liu and co-workers who called it 'cage water' [4]. The ice form structure is also observed in other clusters having large numbers of water molecules. Zwier and co-workers investigated benzene-$(H_2O)_n$ clusters by IDIR spectroscopy and found that the cluster with $n = 8$ has a structure in which a cubic $(H_2O)_8$ ice is bound to benzene via a π-hydrogen bond [10].

2.3. *Phenol-$(H_2O)_n$ in the S_1 state*

It is known that the acidity of phenol increases drastically by the electronic excitation from S_0 ($pK_a = 9.8$) [21] to S_1 ($pK_a = 4.0$) [22]. Thus, the H-bond strength becomes much stronger and a much larger frequency reduction of ν_{OH} is expected in the S_1 state. The method of observing the IR dip spectrum for the electronic excited cluster was described in the previous section. The fluorescence lifetime of the 0^0 level of bare phenol has been reported to be 2 ns and those of the phenol-$(H_2O)_n$ clusters are 6–18 ns depending on the size [17].

Figure 6 shows the FDIR spectra of phenol-H_2O observed at three different delay times: (a) the IR pulse is introduced 50 ns prior to the UV pulse. The spectrum represents the IR spectrum of S_0 and the dips at 3524 and 3748 cm^{-1} are assigned to phenolic ν_{OH} and ν_3 of H_2O, respectively, in S_0. (b) The IR pulse is introduced with no delay time from the UV pulse. As can be seen in the figure, a new intense band appears at 3388 cm^{-1}. (c) The IR pulse is introduced 5 ns after the UV pulse. The band at 3524 cm^{-1} completely disappears, while the band at 3388 cm^{-1} remains. The band at 3388 cm^{-1} is assigned to the phenolic ν_{OH} in S_1.

Figure 7 shows the FDIR spectra of ν_{OH} of phenol-H_2O and phenol-$(H_2O)_3$ in S_1 and S_0 [13]. As for bare phenol and phenol-$(H_2O)_2$, we could not observe their FDIRS spectra of S_1, because of the short lifetime (2 ns) for bare phenol and of the fast

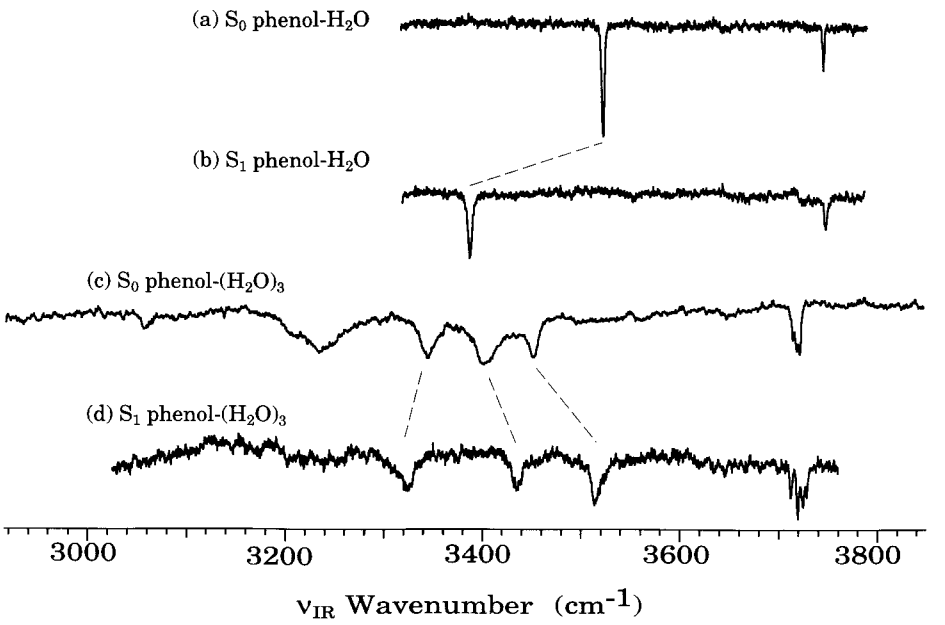

Figure 7. (*a*),(*c*) FDIRS spectra of phenol-$(H_2O)_{n=1,3}$, showing the ν_{OH} vibration in S_0. (*b*), (*d*) FDIRS spectra of phenol-$(H_2O)_{n=1,3}$, showing the ν_{OH} vibration in S_1.

relaxation for phenol-$(H_2O)_2$ [13,17]. The ν_{OH} frequency of phenol in S_1 is reported to be 3581.4 cm^{-1} by Bist and co-workers [23]. From the obtained frequency of ν_{OH} of phenol-H_2O in S_1 (3388 cm^{-1}), the red-shift associated with the H-bond formation is found to be 193 cm^{-1}. This value is 1.45 times larger than that of S_0 (133 cm^{-1}), indicating the increase of the proton donating ability of phenol in S_1. The vibrational frequency of ν_3 of H_2O, which is the proton acceptor, is 3748 cm^{-1}. This value is the same as that for S_0 within the experimental accuracy and it is concluded that the H_2O site is almost unchanged upon the electronic excitation of phenol.

Although a theoretical calculation of the clusters in S_1 has not been performed, the geometrical structure of phenol-$(H_2O)_3$ in S_1 is thought to be a ring form similar to that of S_0. This is because the S_1–S_0 electronic spectrum of phenol-$(H_2O)_3$ shows an intense 0,0 band followed by a short progression, suggesting a small change in the intermolecular conformation [16]. Figure 7(*d*) shows the IR spectrum of phenol-$(H_2O)_3$ in S_1. As seen in the figure, three H-bonded ν_{OH} bands at 3325, 3435 and 3514 cm^{-1} are widely separated compared to the corresponding bands in S_0, and one H-bonded ν_{OH} band is missing in S_1. The bands at $\sim$ 3720 cm^{-1} are assigned to ν_{OH} free from the H-bond similar to those in the spectrum of S_0 (figure 7(*c*)). The observed larger splitting among the H-bonded ν_{OH} in the ring is described by an increase in the interaction between the ν_{OH} vibrations associated with the increase in acidity. As seen in figure 7(*c*), the lowest frequency ν_{OH} in S_0 is very broad. The corresponding band in S_1 may become so broad that it may be smeared on observation.

It was found that the increase in acidity of phenol in S_1 drastically affects the structure of phenol-$(H_2O)_2$. As seen in figure 3, the electronic spectrum of phenol-$(H_2O)_2$ at 36230 cm^{-1} is very broad. The dispersed fluorescence spectrum observed after exciting the band shows only the broad structure which is attributed to the intra-cluster vibrational redistribution (IVR) [13]. The results clearly indicate the broad band peak at 36230 cm^{-1} is not the 0,0 band of phenol-$(H_2O)_2$ and the 0,0 band is

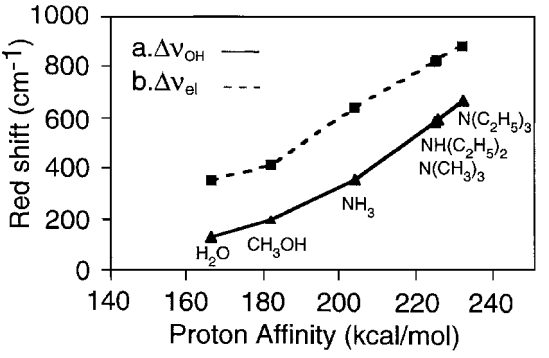

Figure 8. Plot of the red shifts of S_1–S_0 transition frequency and phenolic ν_{OH} versus proton affinity of acceptor of the H-bonded 1:1 clusters of phenol.

thought to have a very small Franck–Condon factor. Phenol-$(H_2O)_2$ is the smallest cluster among the ring form clusters and may have a strain in the H-bond ring. The electronic excitation of phenol moiety may induce a deformation of the stressed ring-form, resulting in a geometrical change such as a H-bond cleavage.

2.4. *OH frequency shift and proton affinity*

The correlation between the red shift of the ν_{OH} frequency of the proton donating site and the proton affinity (PA) of the proton accepting site has been investigated extensively in the condensed phase. We investigated the same relationship for a phenol-base (1:1) cluster, where the base molecules are H_2O, CH_3OH, NH_3 and amines. The IDIRS have been performed for these clusters. Figure 8 shows the plot of the observed red shifts ($\Delta\nu_{OH}$) of ν_{OH} versus PA of the base [24]. Also the red-shift ($\Delta\nu_{el}$) of the S_1–S_0 electronic transition is plotted. As seen in the figure, there is an excellent correlation between the red-shift and PA, and the OH bond strength becomes weaker with increasing PA of the base. It should be noted that frequency reduction is as large as 670 cm^{-1} for phenol-triethylamine.

2.5. *Other H-bonded clusters*

2.5.1. *Tropolone-$(H_2O)_n$ and -$(CH_3OH)_n$*

Tropolone is a non-benzenoid aromatic molecule having an intramolecular H-bond between hydroxyl (OH) and carbonyl group, and its double minimum potential has been a matter of interest with respect to tunnelling along the symmetric H atom transfer coordinate [25–30]. The electronic spectrum of jet-cooled tropolone shows a characteristic doublet structure associated with the tunnelling. The tunnelling doublet in the S_1 state has been reported to be about 20 cm^{-1}, while that of the S_0 state was found to be less than 1 cm^{-1} [30]. It has been known that the symmetric double minimum potential of bare tropolone is readily destroyed by cluster formation with other molecule(s), such as water or methanol. Figure 9 shows the electronic spectrum of the origin region of the S_1–S_0 transition of tropolone and its clusters with water molecule(s) [31]. As is seen in the figure, no doublet occurs for the cluster bands, while the doublet splitting of bare tropolone is about 20 cm^{-1}. The result indicates that the intermolecular H-bond formation makes the tunnelling coordinate so asymmetric that the doublet disappears. This implies that there may be competition between the intermolecular and the intramolecular H-bonding associated with the cluster formation.

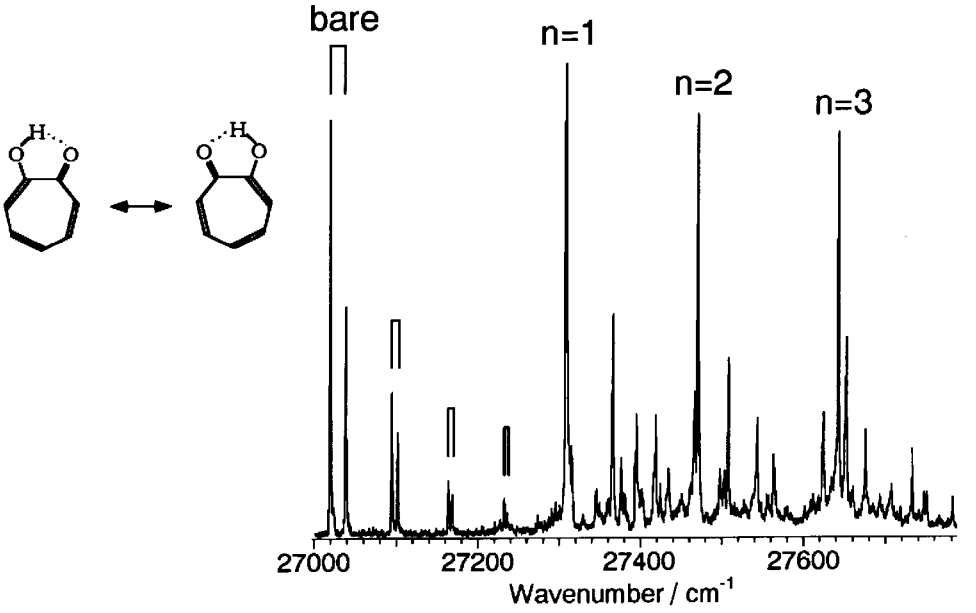

Figure 9. Proton tunnelling of tropolone and S_1–S_0 LIF spectrum of bare tropolone and tropolone-$(H_2O)_n$ clusters in a supersonic jet. Doublet structure of bare tropolone indicates the proton tunnelling splitting.

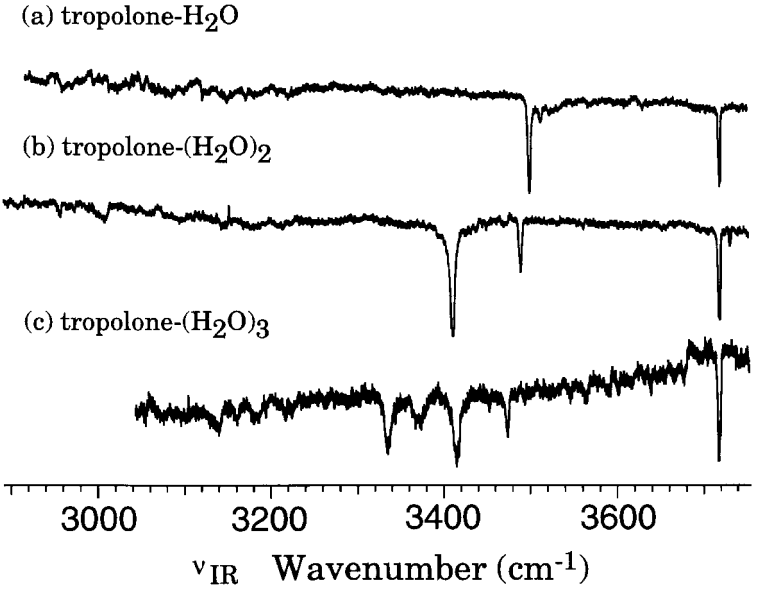

Figure 10. FDIRS spectra of tropolone-$(H_2O)_{n=1-3}$ clusters in the ν_{OH} region.

How many solvent molecules are necessary to break the intramolecular H-bond? Such a change can be investigated by observing the OH vibrations (ν_{OH}). The IR spectra of jet-cooled tropolone and its clusters have extensively been examined by our group [31] and Zwier and co-workers [32]. Figure 10 shows the IR spectra of tropolone-$(H_2O)_n$ for $n = 1$–3 in S_0 [31]. We also observed the IR spectra of tropolone-$(CH_3OH)_n$ for $n = 1$–2, which are shown in figure 11. For the intramolecular H-

Table 1. Vibrational frequencies (cm^{-1}) of tropolone-$(H_2O)_n$ ($n = 1$–3) and tropolone-$(CH_3OH)_n$ ($n = 1$, 2) clusters.

	Non-H-bonded OH	H-bonded OH
Tropolone		3140[a]
Tropolone-H_2O	3722	3520
		3502
Tropolone-$(H_2O)_2$	3731	3490
	3718	3411
Tropolone-$(H_2O)_3$	3718	3475
		3415
		3375
		3334
Tropolone-CH_3OH		3502
Tropolone-$(CH_3OH)_2$		3436
		3384

[a] From [32].

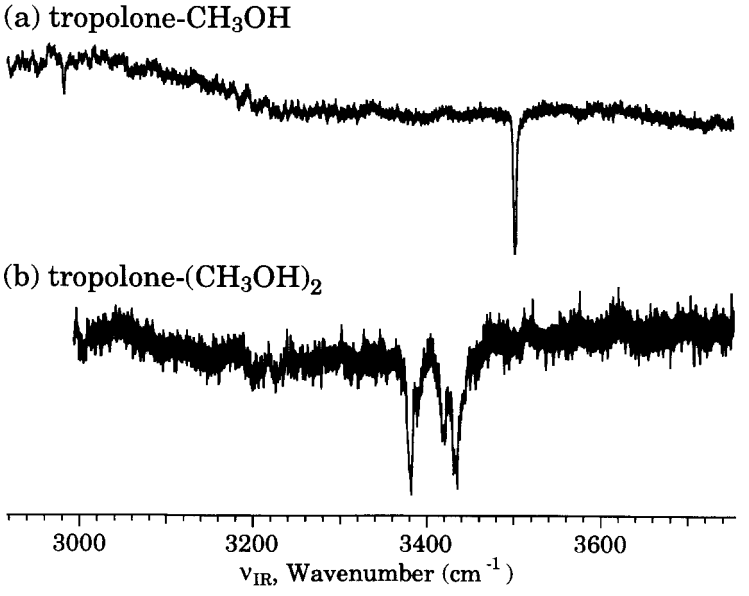

Figure 11. FDIRS spectra of tropolone-$(CH_3OH)_{n=1,2}$ clusters in the ν_{OH} region.

bonded ν_{OH} of bare tropolone, Zwier and co-workers observed a weak ν_{OH} band at 3140 cm^{-1} [32]. The frequencies of the observed bands are listed in table 1. The bands are classified into two groups; one is due to the sharp bands appearing at 3720± 2 cm^{-1} which are very close to the ν_3 band of a water molecule. The bands belonging to this group are due to OH oscillators free from H-bonds, so that they may be called 'H-bond free OH vibrations' or 'dangling OH vibrations'. This assignment is confirmed from the result that no corresponding band appears in the spectra of tropolone-$(CH_3OH)_n$, because there is no dangling OH oscillator in these clusters. The other group are prominent bands appearing in the lower frequency region, and the bands are assigned to the H-bonded OH stretches. Thus, the spectra in figure 10 exhibit the 'window' region between the two groups, which suggests ring forms similar to the case of phenol-$(H_2O)_n$. However, there is a slight difference between phenol-$(H_2O)_n$ and

tropolone-$(H_2O)_n$. In the ring form phenol-$(H_2O)_n$ clusters, all the H-bonded ν_{OH} including phenolic ν_{OH} appear in the region between 3200 and 3600 cm^{-1}, so that there is a sharp propensity with respect to the number of H-bonded OH bands in their IR spectra; $(n+1)$ bands appear in the H-bonded OH region of the clusters with $n = 1$.

However, it is noticed that only two bands are associated with tropolone-$(H_2O)_2$, as shown in figure 10(*b*), being different from the case of the phenol-$(H_2O)_n$ clusters. The difference is that the OH band due to the tropolone moiety does not appear in both spectra, indicating that the intramolecular H-bond of the OH oscillator in both species is still preserved for a size of $n = 1$ and 2. On the other hand, the spectrum of tropolone-$(H_2O)_3$ shown in figure 10(*c*) exhibits four intense bands in the region of the H-bonded OH stretches. In this respect the spectrum of tropolone-$(H_2O)_3$ is very similar to that of phenol-$(H_2O)_3$ which has been known to be the ring H-bonding conformation. Therefore, the spectrum shows that there must be four H-bonded OH groups in the $n = 3$ cluster, suggesting that the intramolecular H-bond of the tropolone site is destroyed by the intermolecular H-bond formation and the ring form is associated with their intermolecular H-bonds. The similar size-dependence is observed for the IR spectra of tropolone-$(CH_3OH)_n$, in which the $n = 2$ cluster shows the break of the intramolecular H-bond. Since proton affinity (PA) of CH_3OH (185 kcal mol^{-1}) is larger than that of H_2O (165 kcal mol^{-1}), it is reasonable that the breaking of the intramolecular H-bond takes place in the smaller size tropolone-$(CH_3OH)_n$, rather than tropolone-$(H_2O)_n$. Further work showing the disappearance of the intramolecular H-bonded OH would provide conclusive evidence for the breakdown of the intramolecular H-bond by the intermolecular H-bond formation.

Although the spectra strongly suggest the ring conformation for the $n = 3$ and $n = 2$ for the tropolone-$(H_2O)_n$ and $(CH_3OH)_n$ systems, theoretical calculations by using *ab initio* methods do not give conclusive results for a stable ring conformer. Even for tropolone-H_2O, the calculated results predict that a few isomers are equally feasible in respect of the stabilization energy [32]. The difficulty seems to arise from the fact that the stabilization energy of the clusters involving an intramolecular H-bond is quite fragile, compared to those bound by intermolecular H-bonds only.

2.5.2. $(Phenol)_{n=2,3}$

Phenol dimer and trimer are thought to be basic units of the phenol crystal whose structure is known to be pseudo-orthorhombic [33,34]. Their structures and dynamics, thus, provide important information for studies of crystal growth and vibration-phonon coupling in the crystal. Fuke and Kaya first reported the electronic spectra of the phenol dimer and the trimer in supersonic jets [35]. Later, Connell and co-workers obtained the rotational constants of the dimer by rotational coherence spectroscopy and reported that two phenols are bound by a single H-bond [36]. For the trimer, Fuke and Kaya suggested a ring structure for the trimer based on the electronic spectrum. However, no direct evidence of a cyclic structure has yet been given. If the structure of the trimer is of ring form, it must belong to a symmetry group involving a three-fold axis, for example the C_3 point group. Therefore, an intensity alternation between IR and Raman spectra will be observed for the three ν_{OH} vibrations if the trimer is of ring form.

Figure 12 shows the IDIRS and IDSRS spectra of ν_{OH} of (a) bare phenol, (b) and (c) phenol dimer, and (d) and (e) phenol trimer [37]. In the phenol dimer, two ν_{OH} bands were observed: one located at 3654 cm^{-1} and the other at 3530 cm^{-1}. The red-shifts of these vibrations from that of the bare phenol (3657 cm^{-1}) are 3 and 127 cm^{-1},

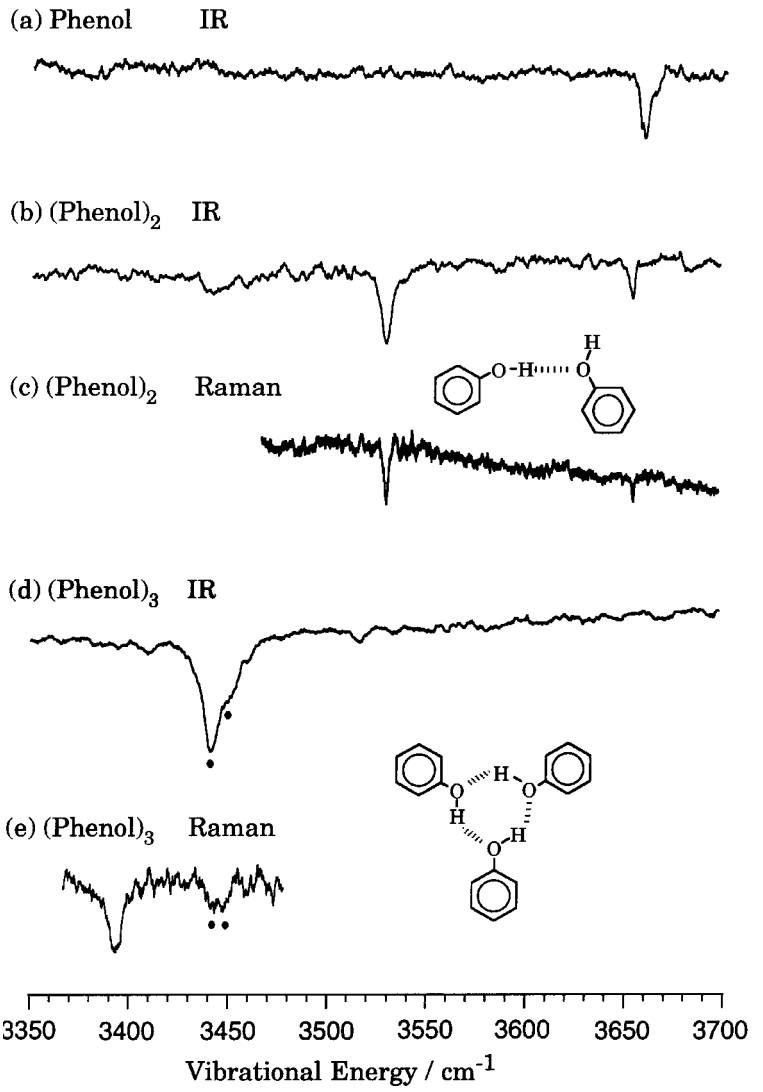

Figure 12. IDIRS spectrum of bare phenol, and IDIRS and IDSRS spectra of $(phenol)_{n=2,3}$ clusters.

respectively. The observed frequencies agree well with those observed by Hartland and co-workers with Raman spectroscopy [6]. The former band is assigned to ν_{OH} of the proton-accepting phenol and the latter band to ν_{OH} of the proton-donating phenol.

In the IR spectrum of the trimer (figure 12 (d)), two ν_{OH} bands are observed at 3441 and 3449 cm^{-1}. The latter band is seen at a shoulder of the former band. The red shifts of the two bands are 216 and 208 cm^{-1}, respectively, which are further red shifted from those of the dimer. The other noticeable feature of the spectrum is that no band is seen in the region near 3660 cm^{-1}, which is the frequency expected for ν_{OH} free from the H-bond. This result indicates that all three OH groups are involved in H-bonds in the trimer, and consequently that the trimer is of ring form.

Since the ring form trimer, shown in figure 12, has a C_3 axis, it may belong to the C_3 point group assuming that the orientation of the aromatic ring does not affect ν_{OH}

significantly. In this group, the three in-plane phenolic ν_{OH} vibrations are classified into A and E symmetry species. The A symmetry vibration is Raman active but IR inactive. The E symmetry vibrations are weak in Raman but active in IR. The IR and Raman spectra of the phenol timer in figures 12(*d*) and 12(*e*) clearly show the expected intensity alternation. As seen in the Raman spectrum (figure 12(*e*)), the bands at 3441 and 3449 cm^{-1} observed in the IR spectrum weakly appeared, while an intense band has appeared at 3394 cm^{-1}. These results agree very well with the expectation for the ring form trimer. Therefore, it is concluded that (i) the phenol trimer is of ring form, (ii) the 3394 cm^{-1} vibration observed in the Raman spectrum is the symmetric (A species) OH stretching vibration and (iii) the vibrations of 3441 and 3449 cm^{-1} observed in the infrared spectrum are the nearly degenerate (E species) OH stretching vibrations.

To confirm the assignments given above, the Raman depolarization ratios (ρ) for the three OH stretching vibrations were measured [37]. The depolarization ratio is obtained as the ratio of the Raman dip intensities ($\mathbf{I}_{\perp}/\mathbf{I}_{//}$) measured when the direction of the two linearly polarized Raman pumping beams are perpendicular ($\mathbf{E}_1 \perp \mathbf{E}_2$) and parallel ($\mathbf{E}_1 // \mathbf{E}_2$). The direction of the polarization was changed by use of a Babinet Soleile compensater which was introduced in one of the Raman pumping (second harmonics of Nd:YAG laser) laser beams. The measurements were performed under the condition that the spectra were not saturated by Raman pumping lasers. Also, care was taken to correct for the reflection efficiency of the beam combiner for the two laser beams with different polarization. The obtained ρ values were 0.17 ± 0.05 for the 3394 cm^{-1} band and 0.7 ± 0.1 for the 3441 and 3449 cm^{-1} bands. Since the ratio ($\rho = \mathbf{I}_{\perp}/\mathbf{I}_{//}$) is $0 \leqslant \rho < 0.75$ for totally symmetric vibration and $\rho = 0.75$ for the non-totally symmetric vibration, the former band is assigned to the totally symmetric vibration and the latter to the non-totally symmetric vibrations. Therefore, the ring structure of the trimer is confirmed by the measurement of the Raman depolarization ratios.

2.5.3. *Fluorobenzene-$(CH_3OH)_{n=1,2}$: precursors for nucleophilic substitution reactions*

One of the important aspects of clusters from a view point of chemical interest is the intracluster reactions initiated by photo-excitation or photo-ionization. An intracluster nucleophilic substitution (S_N) reaction is a typical example. The nucleophilic substitution reaction occurring in van der Waals clusters was first found by Brutschy and co-workers, for the C_6H_5F(FB)-CD_3OD system [38].

Figure 13(*a*) shows the origin region of the S_1–S_0 fluorescence excitation spectrum of FB-$(CH_3OH)_n$ [39]. The cluster bands appear in the blue-side of the 0–0 band of bare FB at 37816 cm^{-1}. The mass-selected REMPI spectra of the same region are shown in figures 13(*b*)–(*d*). From figure 13(*d*), it is evident that the ionization of the clusters denoted by 1, 2, 5 and 6 produces $C_6H_5OCH_3^+$, which is the product of the S_N reaction, while the clusters denoted by 3 and 4 do not. Brutschy and co-workers assigned bands 3 and 4 as due to FB-(CH_3OH), the bands 5 and 6 are FB-$(CH_3OH)_2$, and the bands 1 and 2 are FB-$(CH_3OH)_3$. They concluded that the reaction takes place from the clusters with $n \geqslant 2$ by the following reaction,

$$[C_6H_5F\text{-}(CH_3OH)_n]^+ \rightarrow C_6H_5OCH_3^+ + HF + (CH_3OH)_{n-1}.$$

In addition to the size dependence, Maeyama and Mikami suggested that a specific orientation in the clusters may be also important for the reaction to occur [40]. Thus, vibrational spectroscopy have been applied to investigate the relationship between the structure and the reactivity.

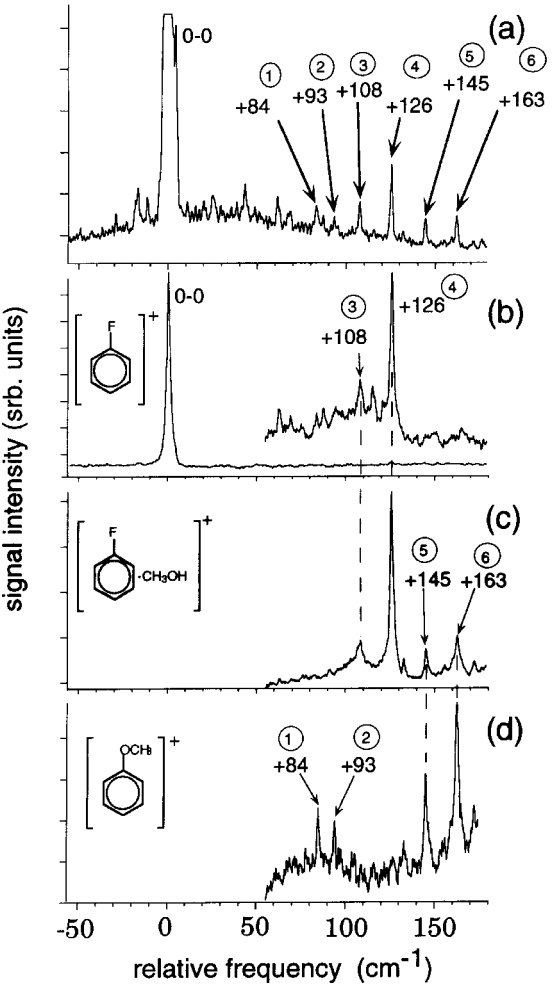

Figure 13. (*a*) S_1–S_0 LIF spectrum of bare FB and FB-$(CH_3OH)_n$ clusters in a supersonic jet. (*b*)–(*d*) mass selected REMPI in the same energy region.

Figure 14 shows FDIRS spectra of FB-$(CH_3OH)_n$ in the 2900–3800 cm^{-1} region. Since each methanol has one OH oscillator, the number of the ν_{OH} bands in the IR spectrum is thought to be equal to that of methanol molecules in the cluster. In figure 14(*a*), the FDIRS spectrum obtained by fixing ν_{UV} to the band 4 in figure 13 shows a sharp band at 3661 cm^{-1}, which is assigned to ν_{OH} of the methanol site. The bands in the 2900–3100 cm^{-1} region are assigned to ν_{CH} of the methanol and the FB sites. Thus, it is concluded that cluster 4, which is non-reactive, is the $n = 1$ cluster, that is FB-CH_3OH. The red shift of ν_{OH} from bare methanol is 20 cm^{-1}. This shift is much smaller than that of the H-bonded cluster of phenol described previously. This small shift indicates that the cluster has the structure that the OH group of methanol is H-bonded on the phenyl ring of FB, so called a π-complex. An *ab initio* calculation with the HF-SCF/6-31G(dp) level also suggested the π-complex structure [39].

For FB-$(CH_3OH)_2$, three isomers are identified from the IR spectra. The IR spectra of the reactive clusters 5 and 6 (figures 14(*b*) and 14(*c*)), show two intense ν_{OH}

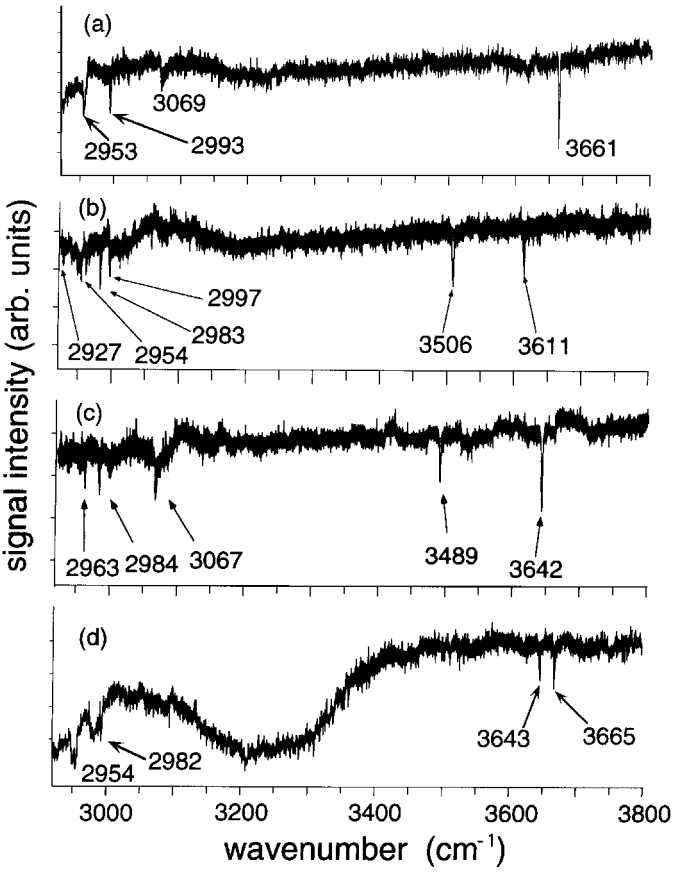

Figure 14. FDIRS spectra of FB-$(CH_3OH)_{n=1,2}$ obtained by fixing the UV frequencies to the peaks observed in figure 13 (*a*); UV frequency is fixed to (*a*) peak 4, (*b*) peak 5, (*c*) peak 6, and (*d*) peak 3, respectively.

bands and thus they are assigned to isomers of FB-$(CH_3OH)_2$. The IR spectrum of non-reactive cluster 3 also exhibits two ν_{OH} bands (figure 14(*d*)). The difference between the reactive and non-reactive species can be recognized by their IR spectra. The red-shift of the lower frequency ν_{OH} band of the reactive isomers 5 and 6, is much larger than that of the non-reactive isomer 3.

It was found that the IR spectra of the isomers 5 and 6 have a feature similar to that of the bare methanol dimer, $(CH_3OH)_2$. The IR spectrum of $(CH_3OH)_2$ measured by Huisken and co-workers [2] shows two ν_{OH} bands at 3684 and 3574 cm^{-1}. The lower frequency band is assigned to ν_{OH} of the proton donor site and the higher band to ν_{OH} of the acceptor site. The separation of the two bands of bare $(CH_3OH)_2$ is 110 cm^{-1}, which is similar to that of clusters 5 (95 cm^{-1}) and 6 (153 cm^{-1}). Thus, the clusters are thought to have a structure where the methanol dimer is bound to the phenyl ring of FB by a π-type H-bond. The low frequency ν_{OH} bands in the clusters are assigned to ν_{OH} of the proton donating methanol in the dimer, and the higher frequency bands are attributed to the proton accepting methanol in the dimer.

For isomer 3, two ν_{OH} bands appear close to each other and their frequencies are similar to that of the ν_{OH} band of the $n = 1$ cluster (figure 14(*d*)). Such a small frequency separation indicates that each methanol molecule is bound to the phenyl

plane from a different side by a π-type H-bond. The isomer dependence of the S_N reaction in the FB-$(CH_3OH)_2$ clusters clearly demonstrates that the methanol dimer structure is necessary for the reaction to occur after ionization. The non-reactivity of the $n = 1$ cluster is also explained by the same reasoning.

As to the clusters 1 and 2, which also produce the reaction product, the IR spectra could not be obtained because the S_1–S_0 fluorescence signal is too weak to observe. Brutschy and coworkers are also performing IR spectroscopic work of the higher clusters [41].

3. Cluster ions

3.1. *Infrared multiphoton dissociation (IRMPD) spectroscopy*

The first gas phase IR spectroscopy of H-bonded cluster ions was performed by Schwarz for hydrated hydronium ions, $H_3O^+(H_2O)_n$ [42]. The cluster ions were produced by pulse radiolysis of water vapour and IR absorption was directly measured in the OH stretch region, so that the size selection was insufficient. Most modern IR studies of H-bonded cluster ions share the framework of IR multiphoton dissociation (IRMPD) spectroscopy developed by Lee and co-workers [1]. In this method, mass-selection of cluster ions is carried out by using electric and/or magnetic fields. IR multiphoton dissociation is utilized for sensitive detection of the IR absorption of mass-selected cluster ions. Because the H-bond strengths are greatly enhanced with ionization, two or more IR photons are needed to break the intermolecular bond(s) in cluster ions. The absorption of the first IR photon is considered to be a bottleneck in the multiphoton process, because the near-resonance effect due to high vibrational density is expected in the successive photon absorption. Therefore, when the IR wavelength is tuned to the resonance with the vibrational transition of interest, the multiphoton dissociation cross-section is greatly enhanced.

In the IRMPD spectroscopic experiment of Lee and co-workers, cluster ions produced in a corona discharge source were first mass-selected by a sector magnet. The mass selected ions were injected into an octapole beam guide used as an ion trap, into which the IR laser beam was introduced for multiphoton dissociation. Produced fragment ions were mass-selected again, and were detected by an ion detector. IR spectra of cluster ions were measured by scanning the wavelength while monitoring the yield of the dissociation fragments. When the cluster size was so small that the vibrational density was not enough to induce the multiphoton absorption, in addition to tunable IR light, an intense CO_2 laser was used to assist dissociation of the cluster ions. They observed the OH stretches of the hydrated hydronium ions [1], and proved the *ab initio* calculated structures in which the hydronium ion resides at the center of the clusters, surrounded by a solvation shell of water molecules. They also measured the spectra of ammoniated ammonium ions, $NH_4^+(NH_3)_n$ [43], and of various protonated ion–water clusters by using this method [44].

Several other groups also carried out IRMPD spectroscopy of various cluster ions. Lisy and co-workers measured IR spectra of solvated metal ions such as $Cs^+(CH_3OH)_n$ by monitoring the depletion yield of the parent ions [45]. Recently they developed a triple quadrupole mass spectrometer for IRMPD spectroscopy. In this apparatus, cluster ions were mass-selected at the first quadrupole filter, and irradiated by IR light in the second filter, which was operated only with the electric potential with radio frequency (RF) and served as an ion guide. Fragment ions were mass-selected in the third filter, and were detected. They applied this apparatus to observe the 3 μm region of the solvated metal ions, and discussed the size dependence of H-bond formation among the solvent molecules, and predicted the presence of several structural isomers

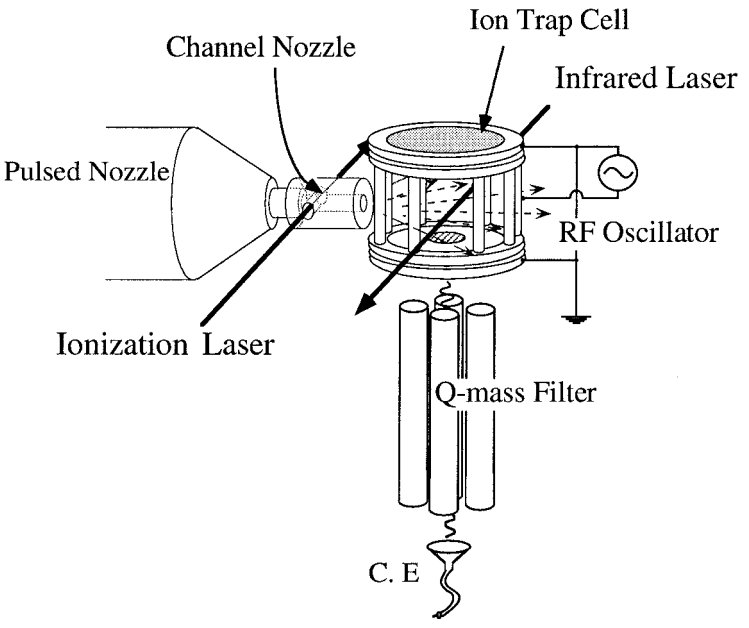

Figure 15. Experimental apparatus for RF trapped ion infrared multiphoton dissociation spectroscopy.

[46]. Kondo and co-workers also constructed a tandem mass filter apparatus [47]. They employed a serpentine octapole ion guide in the interaction region with IR light, and measured ν_2 vibrations of $NH_4^+(NH_3)_n$. They proved a shell structure of the cluster ions by comparing the observed spectra with those calculated.

Reflectron type time-of-flight mass spectrometers can also be utilized for IRMPD spectroscopy of cluster ions. Fragment ions produced by IR absorption are separated from parent ions by using a reflectron energy analyser, and are detected. Okumura and co-workers observed the OH stretch region of $NO^+(H_2O)_n$ clusters, and found that an intracluster reaction resulting in $H_3O^+(H_2O)_{n-1}(HONO)$ production occurs at the $n >$ 3 cluster [48]. Much simpler IRMPD spectroscopy was proposed by Nakanaga *et al.* [49]. They used the same experimental apparatus as IR–UV double resonance spectroscopy of neutral clusters (see section 2.1), but introduced the ionization light prior to the IR light. IR absorption of cluster ions was detected as depletion of the cluster ions due to multiphoton dissociation. They showed production of cold aniline-Ar_n cluster ions with REMPI of the corresponding neutral clusters. This method is useful for small size cluster ions which are easily produced by REMPI.

The IRMPD technique has also been applied to high resolution spectroscopy. Maier and co-workers observed rotationally resolved NH stretching vibrations of NH_2^+-rare gas cluster ions [50]. The precise structures of the radical cluster ions were determined.

The authors' group also developed an IRMPD spectroscopic technique called RF trapped ion IR multiphoton dissociation spectroscopy [51, 52]. Figure 15 shows its experimental apparatus. In this method, we combine a channel nozzle system for the efficient generation of cluster ions with a Paul-type ion trap. The trap is used for size selection as well as for ion storage, and makes the apparatus simpler. A gaseous mixture of helium with vapours of solute and solvent is expanded through a pulsed nozzle with a channel orifice. The channel orifice has a side hole, which crosses with the

channel at right angles. A UV laser beam is focused into the side hole, so that solute molecules are photoionized at the crossing point. The laser wavelength is fixed to the electronic transition of the solute molecule. The cluster ions are formed by collision among solute ions, solvent molecules and helium atoms in the collision region of the channel. The cluster ions are cooled down through expansion into vacuum. For the preparation of cluster ions this method is much more efficient, because no fragmentation takes place in the generation process, while direct photoionization of neutral clusters in the jets is usually accompanied by extensive fragmentation [53].

Cluster ions cooled by the expansion from the nozzle are introduced to a cylindrical ion trap cell. The cell is the so-called Paul-type trap, and is composed of a cylindrical cage electrode and two end-caps used as the other electrode. An RF electric potential is applied to the cylindrical cage electrode with respect to the grounded end-cap electrode. The phase of the RF field is properly adjusted to be synchronized with the ionization laser pulse. This phase locking is effective in increasing the trap efficiency of the ions. The mass selection of cluster ions is performed by adjusting an appropriate voltage and frequency of the RF potential. The cluster ions of interest are trapped in the cell by a suitable condition of the RF potential, and the other cluster ions are removed from the cell during storage. After about 1 ms storage, a tunable IR light beam, whose wavelength is scanned, is introduced into the trap cell. The photodissociation fragments are spontaneously ejected from the trap cell. Then, they are mass-selected by a quadrupole mass filter, and are detected by a channel multiplier. The ion current is amplified and is recorded by a boxcar integrator and computer. Several results obtained by the RF trapped ion IR multiphoton dissociation spectroscopy are introduced in following sections [51, 52].

3.2. *Drastic change in hydrogen-bonded structure induced by ionization*; $(phenol)^+_{n=2-4}$

The most significant feature of H-bonded cluster ions is an increase of their H-bond strength. In the ionic state of typical H-bonded clusters, the H-bond strength increases as much as twice of those of the corresponding neutral clusters, which are in the range of 5–10 kcal mol^{-1}. Such a drastic increase of the bond strength upon ionization of a neutral cluster leads to a large change in the cluster structure. In a previous section describing the neutral $(phenol)_n$ clusters (section 2.5.2), we showed that the neutral dimer, $(phenol)_2$, has the non-cyclic form in which one acts as an acceptor and the other is a donor with respect to the H-bond structure. Also we demonstrated that the neutral trimer exhibits the ring form having cyclic H-bonds. In this section, we examine the structure of their ions by using RF trapped ion IR multiphoton dissociation spectroscopy.

Figure 16 shows IRMPD spectra of (a) $(phenol)^+_2$ (b) $(phenol)^+_3$ and (c) $(phenol)^+_4$, respectively [52]. Mass spectra of the cluster ions trapped in the cell are reproduced in figure 17, indicating that a single ionic species dominates for each trapping condition. Thus, the mass spectra certify that the observed IR spectra in figure 16 (*a*)–(*c*) are due to the size-selected phenol cluster ions. Figure 16 shows characteristic features of the IR spectra of $(phenol)^+_n$: in each spectrum an intense band occurs at 3620 ± 3, 3627 ± 3 and 3632 ± 3 cm^{-1} for $n = 2$, 3 and 4, respectively. On the other hand, no intense band appears in the region of 3600–3000 cm^{-1} but a broad absorption occurs in each spectrum.

By analysing the IR spectrum, the H-bond feature of $(phenol)^+_2$ will be characterized as follows. The OH stretch frequency of the neutral phenol monomer is 3657 cm^{-1} as described in section 2.2.1, and that of the ion is 3534 cm^{-1}, as shown later.

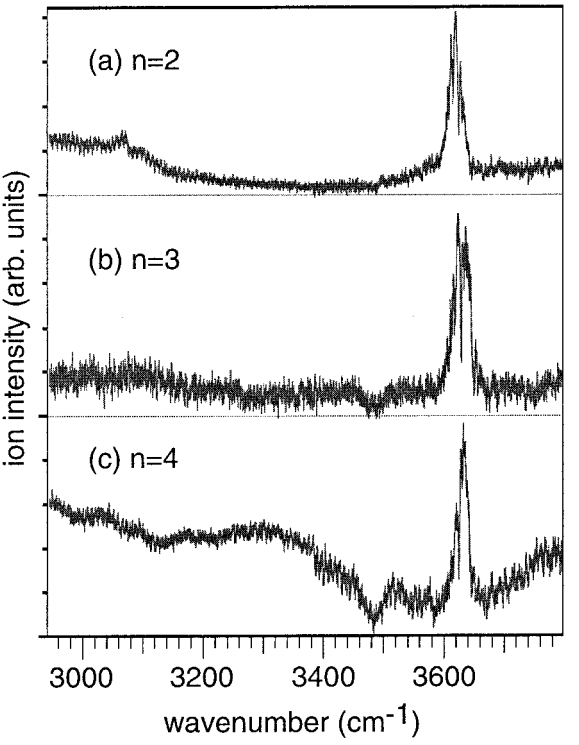

Figure 16. IRMPD spectra of (*a*) $(phenol)_2^+$, (*b*) $(phenol)_3^+$, and (*c*) $(phenol)_4^+$, respectively, obtained by monitoring the $(phenol)_{n-1}^+$ fragment signal as a function of the infrared wavelength.

It is noticed that the dimer ion band at 3620± 3 cm^{-1} is very close to that of the neutral monomer, but is not to that of the ion. The result suggests that the dimer ion band at 3620 cm^{-1} is assigned to the OH stretching vibration of the neutral site which is acting as an acceptor of the hydrogen bond in $(phenol)_2^+$. As a consequence, it is concluded that $(phenol)_2^+$ has an open structure, in which the two phenol sites are inequivalently bound and the charged site appears as a proton donor and the neutral site acts as an acceptor. The H-bond characteristics of $(phenol)_n^+$ for $n = 3$ and 4 are also analysed in the same way as described above. The intense bands at 3627± 3 cm^{-1} for $n = 3$ and 3632± 3 cm^{-1} for $n = 4$ are obviously attributed to the free OH stretching vibrations of the neutral sites, indicating that at least one dangling OH bond is associated with these ions. The presence of the dangling OH bond is an unambiguous evidence that $(phenol)_3^+$ and $(phenol)_4^+$ must have a non-cyclic structure. The non-cyclic form of $(phenol)_3^+$ is in a sharp contrast to the cyclic form of the neutral trimer, $(phenol)_3$, shown in section 2.5.2. The neutral $(phenol)_4$, is also thought to have a ring form structure similar to that of phenol-$(H_2O)_3$ described in section 2.2.2. Thus, the IR spectra of the cluster ions indicate that the intermolecular structures of $(phenol)_3^+$ and $(phenol)_4^+$ are quite different from their corresponding neutral forms, and represent that the cyclic structures are no longer favourable in these ions.

For the non-cyclic $(phenol)_3^+$ and $(phenol)_4^+$, several conformational isomers are possible with respect to their intermolecular H-bonds. Among them, two major candidates of $(phenol)_3^+$, for example, are significant; one is a chain-type form in which three phenol molecules are bound in a linear H-bond chain and the charge is localized

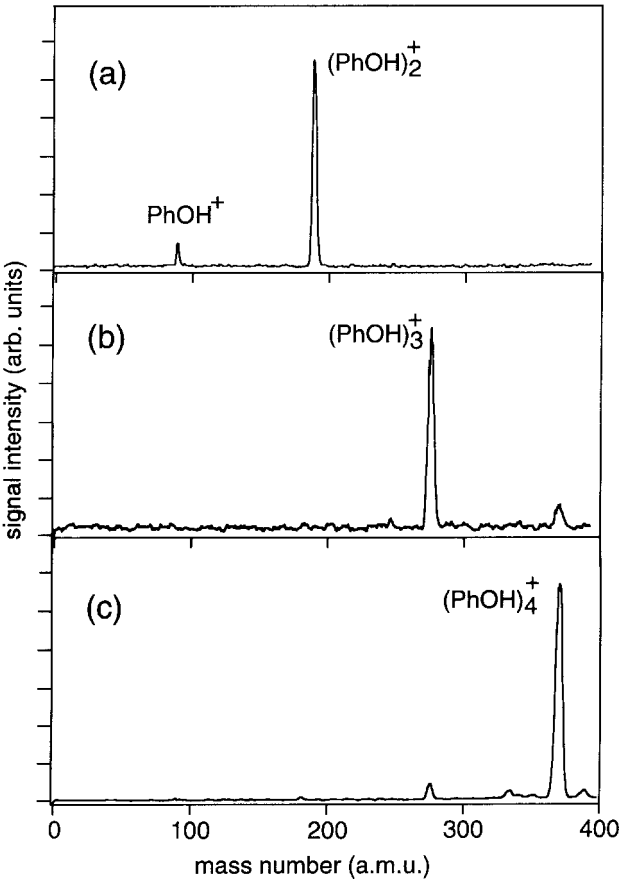

Figure 17. Mass spectra of the cluster ions stored in the trap cell under the different ion trap conditions which are suitable for trapping (*a*) $(phenol)_2^+$, (*b*) $(phenol)_3^+$, and (*c*) $(phenol)_4^+$, respectively. The dominant species in the spectra (*a*)–(*c*) correspond to the IRMPD spectra of figures 16(*a*)–(*c*), respectively.

on one of the three. The other is a sandwich form in which at least two phenyl rings are parallel with each other and the charge is delocalized in the pair of rings. From the IR spectra it is not evident which type of isomer will be feasible. If $(phenol)_n^+$ has the sandwich form, it should show an intense transition in the visible-to-near IR region, which is called the 'charge resonance band' as is well-known for the benzene cluster cations [54]. In order to distinguish the isomer type, we measured the electronic spectra of these cluster ions in this region, and no such strong absorption band was found [52]. From these results we concluded that the chain form is the most consistent as the conformation of the $(phenol)_n^+$ ions.

There are several reasons why such a drastic structure change takes place upon the ionization of the cyclic neutral clusters. It is evident that the number of H-bonds in a cluster with the cyclic form is always larger by one than that in the corresponding isomer with the chain form. For the small-size cyclic clusters, however, all the intermolecular O–H$\cdots\cdots$O bond-angles are expected to be bent. The O–H$\cdots\cdots$O angles in $(phenol)_3$, for example, are necessarily smaller than 180° which is the ordinary H-bond angle between the OH bond and the O atom in the acceptor site. In this respect, the cyclic forms have stress in their intermolecular H-bonds, while the

chain forms do not have such a bond angle strain. Thus, the equilibrium structure of the neutral clusters may be optimized by a trade-off between the additional stabilization due to the extra bond and the destabilization due to the bond angle distortion. In the case of cluster ions, on the other hand, the stabilization energy of a single hydrogen bond involving the ionic moiety is several times larger than that of the neutral site. A large stabilization energy can be obtained by forming a firm bond between the ionic and the neutral moieties. Therefore, the optimization of the intermolecular structure in cluster ions is merely given by forming a dominant hydrogen bond involving the ionic moiety without any bond angle distortion, resulting in the chain forms.

3.3. *Proton transfer in acid–base cluster ions*; $[phenol\text{-}(H_2O)_n]^+$

Proton transfer is one of the most fundamental chemical processes, and plays an essential role in acid–base reactions in solution. In clusters composed of proton donor–acceptor pairs, the cluster-size dependence of the proton transfer is of particular interest in respect of the cluster model of acid–base reactions in solution. The first experimental study on the size dependence of proton transfer was reported by Cheshnovsky and Leutwyler [55] for 1-naphthol-ammonia clusters. It is expected that the enhancement of H-bond strength upon ionization induces not only the drastic structural change but also the intracluster proton transfer reactions. The size-dependence of the proton transfer in the $[phenol\text{-}(H_2O)_n]^+$ cluster ions has been studied by measurements of their electronic spectra [56]. The electronic spectra of the $n \geqslant 3$ cluster ions were very similar to that of the phenoxy radical (C_6H_5O), indicating that these cluster ions have the proton-transferred form which is composed of the phenoxy radical and hydrated hydronium ions;

$$C_6H_5O - H_3O^+(H_2O)_{n-1} \quad (n \geqslant 3).$$

On the other hand, the $n = 1$ and $n = 2$ cluster ions showed broad and structureless spectra which are due to the phenol ion chromophore. This means that proton transfer does not occur in these cluster ions and they are composed of the phenol ion and water molecules;

$$C_6H_5OH^+ - (H_2O)_n \quad (n \leqslant 2).$$

Although the size dependence of the proton transfer in the cluster ions is inferred from their electronic spectra, vibrational spectra of their OH stretching vibrations are expected to provide another evidence for the proton transfer. Figure 18 shows the IR spectra of the $[phenol\text{-}(H_2O)_n]^+$ cluster ions in the region of 2900–3800 cm^{-1} obtained by IRMPD spectroscopy [51]. Figures 18(*a*)–(*d*) show the spectra of the $n = 1$, 2, 3, and $\geqslant 4$ ions, respectively; each of which was obtained by monitoring the intensity of the $[phenol\text{-}(H_2O)_{n-1}]^+$ fragment ion as a function of the IR wavelength. All the spectra show relatively sharp bands in the 3600–3800 cm^{-1} region and an extremely broad one below 3600 cm^{-1}. The sharp bands are assigned to the symmetric (ν_1) and asymmetric (ν_3) OH stretches of the water moiety. The assignments of the broad bands below 3600 cm^{-1} will be discussed later.

In the IR spectrum of the water moiety of the $n = 1$ cluster ion, two intense bands appear at 3625 and 3710 cm^{-1}. These frequencies are very close to those of bare water, of which frequencies of the two OH stretches are 3657 and 3756 cm^{-1}, respectively. On the other hand, the H_3O^+ ion has no fundamental transitions in this region [57,58]. Therefore, the spectrum indicates that the structure of the water moiety is very similar to that of bare water. Consequently, the $n = 1$ cluster ion is considered to have a non-

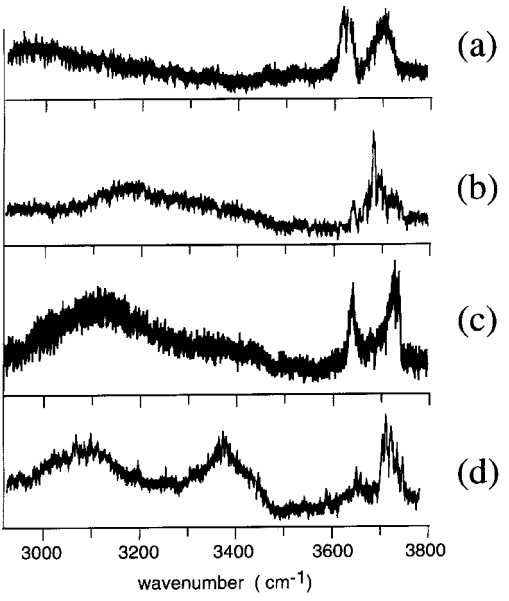

Figure 18. IRMPD spectra of [phenol-$(H_2O)_n$]$^+$: (*a*) $n = 1$, (*b*) $n = 2$, (*c*) $n = 3$, and (*d*) $n \geqslant 4$, respectively. Each spectrum was obtained by monitoring the intensity of the [phenol-$(H_2O)_{n-1}$]$^+$ fragment.

proton-transferred form, [$C_6H_5OH^+$-H_2O]. The infrared spectra of [phenol-$(H_2O)_n$]$^+$ ($n = 3$) also show sharp features consisting of two peaks around 3600 and 3700 cm^{-1}. As was seen in section 2.2.2, the neutral phenol-water clusters of $n = 2$ form the ring structures. The spectral feature of the ring structure is the 'window' region around 3600 cm^{-1}, in which no band occurs. A similar 'window' region should be found for the cluster ions, if they also have the ring forms. This is because the dangling OH stretching frequency is not seriously perturbed with ionization of the phenol site while the larger red-shifts of the H-bonded OH frequencies are expected. However, as seen in figures 18 (*c*) and 18 (*d*), the infrared spectra of [phenol-$(H_2O)_n$]$^+$ ($n \geqslant 3$) show clear bands around 3600 cm^{-1}, and they indicate that the ring structures are not held in the $n \geqslant 3$ cluster ions.

When the proton transfer occurs in the phenol-water cluster ions, the cluster ions can be regarded as being composed of phenoxy radical and hydrated hydronium ions. It has been confirmed that small size hydrated hydronium ions ($n \leqslant 6$) have radial structures in which H_3O^+ is centred and water molecules are bound at each site of H_3O^+ [1]. The structure of the water moiety of the proton-transferred cluster ions is also expected to be radial. In infrared spectra of hydrated hydronium ions, no 'window' region is seen but characteristic bands appear at around 3600 cm^{-1} [1]. These bands originate from the terminal water molecules in the cluster, and are attributed to symmetric OH stretches. The band around 3600 cm^{-1} in the phenol-water cluster ions ($n \geqslant 3$) is considered to have the same origin as the hydrated hydronium ions, and supports the proton transferred form of the cluster ion. For more detailed analyses of the structures, extensive *ab initio* calculations are necessary by using high level methods with large basis sets for the diffuse charge distribution of the cluster ions.

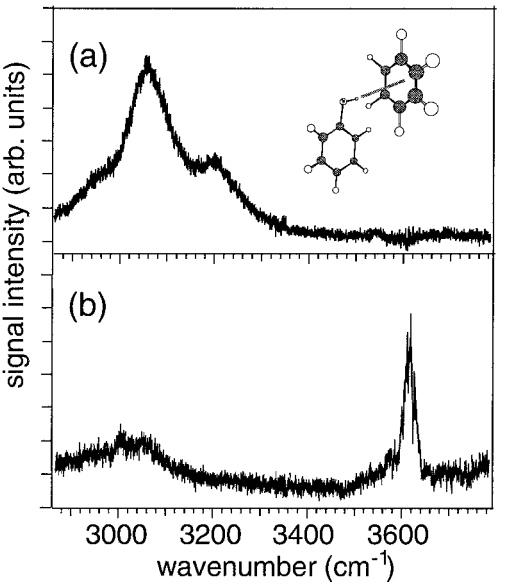

Figure 19. IRMPD spectra of (*a*) (phenol-benzene)$^+$, and (*b*) $(phenol)_2^+$ cluster ions. The spectra were obtained by monitoring the phenol$^+$ fragment intensity as a function of the infrared wavelength. A schematic form of (phenol-benzene)$^+$ is illustrated in (*a*).

3.4. *Large frequency shift of hydrogen-bonded OH vibrations*

In the IR spectra of $(phenol)_n^+$ and [phenol-$(H_2O)_n$]$^+$ shown in figures 16 and 18, it is noticed that only extremely broad absorption occurs in the region 3000–3600 cm^{-1}, where stretching vibrations of the H-bonded OH oscillators should appear. The disappearance of distinct bands in this region is puzzling, because the IR absorption intensity of H-bonded OH oscillators is expected to be much larger than that of the dangling OH oscillators, as seen in section 2.

The IR spectrum of the phenol-benzene hetero dimer ion, (phenol-benzene)$^+$, gives us a key for the interpretation of the broad absorption in $(phenol)_n^+$ and [phenol-$(H_2O)_n$]$^+$ [52]. In figure 19 the spectrum of (phenol-benzene)$^+$ is illustrated. For comparison, the spectrum of $(phenol)_2^+$ shown in figure 16 is also reproduced in the figure. The spectrum of (phenol-benzene)$^+$ shows an intense absorption with a considerably broader feature peaked at about 3060 cm^{-1} with shoulders on its both sides. It is well known that an unsaturated compound with π-electrons, such as benzene, is effective as a proton acceptor, i.e. so-called π-type H-bond. Since the ionization energy of phenol is substantially lower than that of benzene, it is evident that the charge in the hetero dimer ion is localized predominantly on the phenol site. A schematic view of the hetero dimer ion bound by a π-type hydrogen bond between phenol and benzene is illustrated in the inset of figure 19. In this hetero dimer ion, only the OH bond of the phenol ion site appears to be a H-bonded OH oscillator. In this respect, the intense IR band peaked at about 3060 cm^{-1} in figure 19 can uniquely be assigned to the absorption associated with the H-bonded OH stretching vibration of the phenol ion moiety. Since the OH frequency of a bare phenol ion is known to be 3534 cm^{-1}, the difference of about 470 cm^{-1} is considered to be an extremely large red-shift of the OH stretching vibration induced by the π-type H-bond formation of the phenol ion. Thus, such a large frequency reduction, as well as an extremely broad feature, is associated with the hydrogen bond formation in the ionic clusters, even

though the π-type H-bond is substantially weaker than the σ-type H-bond. The result of the (phenol-benzene)$^+$ ion suggests that a much larger frequency reduction and more substantial broadening may easily be expected for the case of σ-type hydrogen bonding systems of phenol ion, such as for $(phenol)_n^+$ and $[phenol\text{-}(H_2O)_n]^+$, and it results in the disappearance of clear structure in the 3000–3600 cm^{-1} region of their IR spectra. Therefore, the broad absorption of these cluster ions below 3600 cm^{-1} is attributed to H-bonded OH stretching vibrations. It is also desirable to perform extensive *ab initio* calculations of these cluster ions for more detailed understanding of the H-bonded OH stretches.

3.5. *Novel techniques for vibrational spectroscopy of molecular ions*

Although IRMPD spectroscopy is a powerful method for studies of cluster ions, there is a difficulty in its application to an ion of a bare molecule, because binding energies of chemical bonds in molecules are usually too large to be dissociated by the vibrational excitation. Despite this difficulty the vibrational spectroscopy of bare molecular ions also has great importance for studies of their clustering processes as standard. Moreover, intramolecular H-bonds in a molecular ion would also be an interesting subject to investigate. One technique to overcome this difficulty is called the 'messenger' method [59–61]. In this method, a van der Waals cluster ion in which a bare molecular ion is weakly bound with a rare gas atom or a H_2 molecule is used instead of a bare ion. IR dissociation spectroscopy can readily be applied to cluster ions which have a weak van der Waals bond. Clustering with a rare gas atom results in a small perturbation to the molecular structure and vibrations of the bare ion, so that the spectrum is expected to be very similar to that of the bare ion. The rare gas atom in the cluster ion plays a role of a 'messenger' of IR absorption for the bare ion. This method was first developed by Lee and co-workers. They used H_2 or Ne as a messenger, and measured IR spectra of the hydrated hydronium ions [59] and the non-classical molecular ion, CH_5^+ [60].

Figure 20 (*a*) shows the IR spectrum of the (phenol-Ar)$^+$ van der Waals cluster ion [61]. The (phenol-Ar)$^+$ ion was produced by REMPI of the (phenol-Ar) neutral cluster, and the depletion of the cluster ion due to predissociation caused by IR absorption was measured. A dip was found at 3535 $\pm$ 2 cm^{-1}, and was assigned to the OH stretch of the cluster ion, which is expected to be very close to the OH stretching of the phenol ion. By using a Kr atom as another messenger, we obtained the OH frequency of the ion to be the same within experimental error ($\pm$ 2 cm^{-1}), confirming that the perturbation of the messenger on the bare ion is actually small.

Although the perturbation due to attachment of a messenger is considered to be very small, sometimes it is not negligible. Lee and co-workers measured IR spectra of hydrated hydronium ions by using both of the messenger and IRMPD techniques [1,59]. The two methods gave spectra which are basically similar to each other. However, the OH stretch of $H_3O^+(H_2O)_2$, for example, showed 80 and 9 cm^{-1} shifts for the H_2 and Ne messengers, respectively. Those large shifts are due to the interaction of the messenger to the OH group of the ion. In the case of (phenol-Ar)$^+$, the precise OH stretch frequency of (phenol)$^+$ is 3534 cm^{-1}, as is shown in the following. The excellent agreement might be due to the structure of the (phenol-Ar)$^+$ cluster ion in which the Ar atom sits on the phenyl group of the ion and is far away from the OH group. Perturbation from a messenger depends on the strength of the interaction and geometry of the cluster.

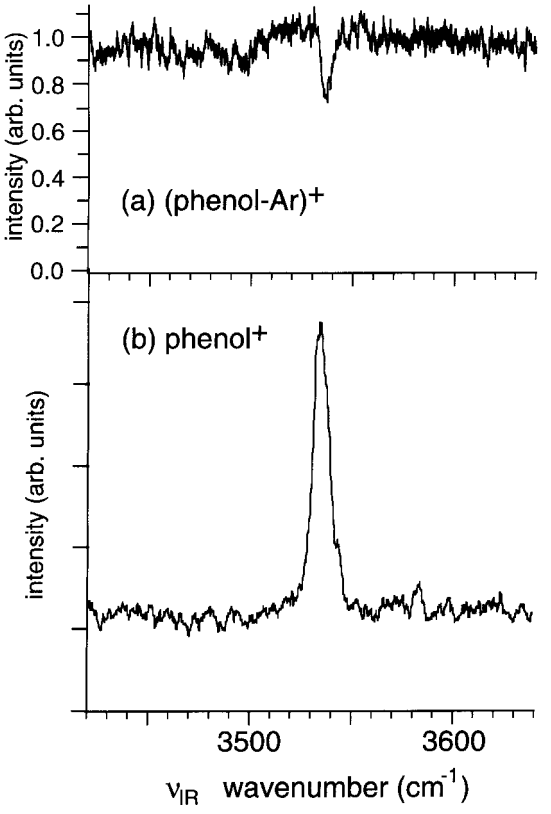

Figure 20. Infrared spectra of the phenol ion in the OH stretching vibrational region obtained by (*a*) the messenger method, and (*b*) autoionization detected infrared spectroscopy, respectively. In spectrum (*a*), the $(phenol\text{-}Ar)^+$ ion was produced by REMPI of the (phenol-Ar) neutral cluster, and the depletion of the cluster ion due to predissociation caused by IR absorption was measured. Spectrum (*b*) was obtained by monitoring the vibrational autoionization signal of high Rydberg states of phenol (see the text).

Recently we proposed a new technique for infrared spectroscopy of bare ions in a supersonic jet [62]. In this technique, we observe vibrational transitions of very high Rydberg states instead of the bare ion. Because of the extremely weak interaction between the ion core and the Rydberg electron, the ion core of the high Rydberg states is regarded as exactly the same as the bare ion. This similarity has been widely confirmed in extensive studies of zero kinetic energy photoelectron spectroscopy (ZEKE-PES) [63]. Since the IR absorption of the Rydberg states is followed by autoionization and the yield spectrum of the resultant ions is observed, we call this new technique autoionization detected infrared spectroscopy (ADIRS). Figure 21 shows the excitation scheme of the method. A jet-cooled neutral molecule is excited to very high Rydberg states (principle quantum number of $n \sim 100$) converging to the vibrationless level ($v = 0$) of the ground state of its ion by using two-colour double resonance excitation via the 0–0 band of the S_1–S_0 transition. An IR laser light excites the ion core of the Rydberg states to the vibrationally excited level ($v = 1$). Because of the vibrational energy of the ion core, the core-excited Rydberg states lie above the first ionization threshold. Energy exchange between the ion core and the Rydberg electron results in spontaneous ejection of the electron, i.e. vibrational autoionization.

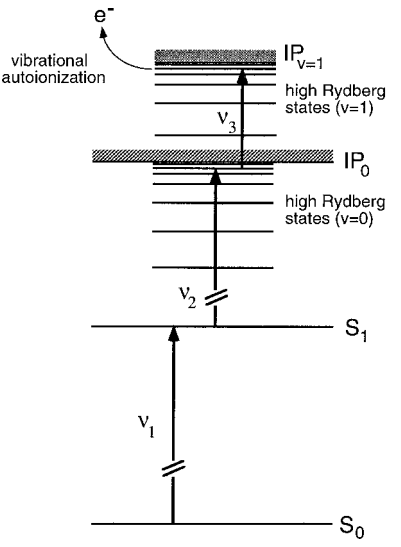

Figure 21. Excitation scheme of autoionization detected infrared spectroscopy (ADIRS).

After an appropriate delay time, a pulsed electric field is applied to the interaction region, and the ions produced by autoionization are extracted into a time-of-flight mass spectrometer. The ions are mass-analysed and detected by an ion detector. Monitoring the autoionization signal, the infrared wavelength is scanned, and infrared spectra are obtained.

Figure 20(*b*) is the ADIR spectrum of $(phenol)^+$ in the OH stretch region [62]. A strong peak is found at 3534 cm^{-1}, and assigned to the OH stretching vibration. This value is almost the same as that obtained by the messenger method. Perturbation from the Rydberg electron to the ion core is much smaller than that from rare gas atoms combined by van der Waals forces. Also the Rydberg states are prepared by two-colour excitation of the jet-cooled molecule so that the rotational temperature in the present method is kept cold. Therefore, the observed frequency 3534 cm^{-1} in ADIRS is expected to be more reliable than that obtained by the messenger method.

The concept of ADIRS, that is use of Rydberg states, is similar with those of ZEKE [63] and photoinduced Rydberg ionization (PIRI) spectroscopy [64]. In the latter, vibrational structure associated with electronic transition are observed, and vibronic bands are restricted by Franck–Condon factors. On the other hand, vibrational transition in ADIRS is restricted by selection rules of the IR absorption ($\Delta v = \pm 1$). Therefore, ZEKE and PIRI spectroscopy is suitable for observation of low frequency vibrations, while ADIRS is powerful for the observation of high frequency modes such as OH and CH stretches. In this regard, these techniques give us complementary information.

4. Concluding remarks

In this review, we presented our results on vibrational spectroscopic studies of H-bonded clusters of organic compounds as well as those ions, emphasizing the characterization of their intermolecular structures. Although the investigations are limited to relatively small small-clusters, it has been demonstrated that local structures of the intermolecular surroundings in size- and/or site-selective clusters are closely related with some of the collective chemical properties in condensed phases. To reach the final goal of our cluster studies, we have to make further effort to characterize the

structure and the dynamical behaviour, such as band shape analyses and observation of time evolution processes involving relaxation, dissociation and evaporation after vibrational excitation. For such study, a time-resolved spectroscopic study of the size-selective clusters will be a next important step, which is now in progress.

Acknowledgements

The authors gratefully acknowledge the support of the Grants-in-Aid for Scientific Researches in Priority Areas (Chemistry of Small Manybody Systems), administered by the Ministry of Education, Science, Culture, and Sports, Japan. The authors also thank all the members of their group past and present who have extensively contributed to the studies presented in this review.

References

[1] Okumura, M., Yeh, L. I., Myers, J. D., and Lee, Y. T., 1986, *J. chem. Phys.*, **85,** 2328; Yeh, L. I., Okumura, M., Myers, J. D., Price, J. M., and Lee, Y. T., 1989, *J. chem. Phys.*, **91**, 7139; Yeh, L. I., Lee, Y. T., and Hougen, J. T., 1994, *J. molec. Spectrosc.*, **164,** 473.

[2] Huisken, F., Kulcke, A., Laush, C., and Lisy, J. M., 1991, *J. chem. Phys.*, **95,** 3924; Huisken, F., and Stemmler, M., 1993, *J. chem. Phys.*, **98,** 7680; Huisken, F., Kaloudis, M., and Kulcke, A., 1996, *J. chem. Phys.*, **104,** 17.

[3] Buck, U., and Meyer, H., 1984, *Phys. Rev. Lett.*, **52,** 109.

[4] Pugliano, N., Cruzan, J. D., Loeser, J. G., and Saykally, R. J., 1992, *J. chem. Phys.*, **98,** 6600; Paul, J. B., Collier, C. P., Saykally, Acherer, J. J., and O'Keefe, A., 1997, *J. phys. Chem.*, **101,** 5211; Liu, K., Brown, M. G., Saykally, R. J., and Clary, D., 1996, *Nature*, **391,** 591.

[5] Escherick, P., and Owyoung, A., 1983, *Chem. Phys. Lett.*, **103,** 235; Escherick, P., Owyoung, A., and Pliva, J., 1985, *J. chem. Phys.*, **83,** 3311; Pilva, J., Escherick, P., and Owyoung, A., 1987, *J. molec. Spectrosc.*, **88,** 393.

[6] Venturo, V. A., and Felker, P. M., 1993, *J. chem. Phys.*, **99,** 748; Shaeffer, M. W., Maxton, P. M., and Felker, P. M., 1994, *Chem. Phys. Lett.*, **224,** 544; Shaeffer, M. W., Kim, W., Maxton, P. M., Romascan, J., and Felker, P. M., 1995, *Chem. Phys. Lett.*, **242,** 632; Hartl and, G. V., Henson, B. F., Venturo, V. A., and Felker, P. M., 1992, *J. phys. Chem.*, **96,** 1164.

[7] Page, R. H., Shen, Y. R., and Lee, Y. T., 1988, *J. chem. Phys.*, **88,** 4621; Page, R. H., Shen, Y. R., and Lee, Y. T., 1988, *J. chem. Phys.*, **88,** 5362.

[8] Riehn, Ch., Lahmann, Ch., Wessermann, B., and Brutschy, B., 1992, *Chem. Phys. Lett.*, **197,** 443; Riehn, Ch., Lahmann, Ch., Wessermann, B., and Brutschy, B., 1992, *Ber. Bunsenges. Physik. Chem.*, **96,** 1161.

[9] Tanabe, S., Ebata, T., Fujii, M., and Mikami, N., 1993, *Chem. Phys. Lett.*, **215,** 347; Mikami, N., 1995, *Bull. Chem. Soc. Jpn.*, **68,** 683; Watanabe, T., Ebata, T., Tanabe, T., and Mikami, N., 1996, *J. chem. Phys.*, **105,** 408; Ebata, T., Fujii, A., Mikami, N., 1996, *Int. J. Mass Spectrosc. Ion Process.*, **159,** 111.

[10] Pribble, R. N., and Zwier, T. S., 1994, *Science*, **265,** 75; Pribble, R. N., and Zwier, T. S., 1994, *Faraday Discuss.*, **97,** 229; Gruenlof, C. J., Carney, J. R., Arrington, C. A., Zwier, T. S., Federicks, S. Y., and Jordan, K. N., 1997, *Science*, **276,** 1678.

[11] Zwier, T. S., 1996, *Annu. Rev. Phys. Chem.*, **47,** 205.

[12] Walther, Th., Bitto, H., Minton, T. K., and Huber, J. R., 1994, *Chem. Phys. Lett.*, **231,** 64.

[13] Ebata, T., Mizuochi, N., Watanabe, T., and Mikami, N., 1996, *J. phys. Chem.* **100,** 546.

[14] Abe, H., Mikami, N., and Ito, M., 1982, *J. phys. Chem.*, **86,** 1768; Oikawa, A., Abe, H., Mikami, N., and Ito, M., 1983, *J. chem. Phys.*, **87,** 5083; Gonohe, N. , Abe, H., Mikami, N., and Ito, M., 1985, *J. phys. Chem.*, **89,** 3642.

[15] Ebata, T., Furukawa, M., Suzuki, T., and Ito, M., 1990, *J. opt. Soc. Am.*, **B7,** 1890.

[16] Berden, G., Meerts, W. L., Schmitt, M., and Kleinermanns, K., 1996, *J. chem. Phys.*, **104,** 972; Schmitt, M., Müller, H., and Kleinermanns, K., 1994, *Chem. Phys. Lett.*, **218,** 246.

[17] Lipert, R. J., and Colson, S. D., 1988, *J. chem. Phys.*, **89,** 4579; Lipert, R. J., Bermudez, G., and Colson, S. D.,1988, *J. phys. Chem.*, **92,** 3801; Lipert, R. J., and Colson, S. D.,1989, *Chem. Phys. Lett.*, **161,** 303; Lipert, R. J. and Colson, S. D., 1990, *J. phys. Chem.*, **94,** 2358.
[18] Stanley, R. J., and Castleman Jr, A. W., 1991, *J. chem. Phys.*, **94,** 7744; Stanley, R. J., and Castleman Jr, A. W., 1993, *J. chem. Phys.*, **98,** 796.
[19] Watanabe, H., and Iwata, S., 1996, *J. chem. Phys.*, **105,** 420.
[20] Matsumoto, Y., Ebata, T., and Mikami, N. (to be published).
[21] Biggs, A. I., and Robinson, R. A., 1961, *J. chem. Soc.*, 338.
[22] Wehry, R. L., and Rogers, L. B., 1965, *J. Am. chem. Soc.*, **87,** 4234.
[23] Bist, H. D., Br and, J. C. D., and Williams, D. R., 1967, *J. molec. Spectrosc.*, **24,** 402.
[24] Iwasaki, A., Fujii, A., Watanabe, T., Ebata, T., and Mikami, N., 1996, *J. phys. Chem.*, **100,** 16053.
[25] Alves, A. C. P., and Hollas, J. M., 1972, *Molec. Phys.*, **23,** 927; Alves, A. C. P., Hollas, J. M., Musa, H., and Ridley, T., 1985, *J. molec. Spectrosc.*, **109,** 99.
[26] Redington, R. L. and Redington, T. E., 1979, *J. molec. Spectrosc.*, **78,** 229; Redington, R. L., Redington, T. E., Hunter, M. A., and Field, R. W., 1990, *J. chem. Phys.*, **92,** 6456; Redington, R. L., and Bock, C. W., 1991, *J. phys. Chem.*, **95,** 10284.
[27] Tomioka, Y., Ito, M., and Mikami, N., 1983, *J. phys. Chem.*, **87,** 4401.
[28] Sekiya, H., Nagashima, Y., and Nishimura, Y., 1990, *J. chem. Phys.*, **92,** 5761; Tsuji, T., Sekiya, H., Nishimura, Y., Mori, A., and Takeshita, H. J., 1991, *J. chem. Phys.*, **95,** 4802; Sekiya, H., Hamabe, H., Ujita, H., Nakano, N., and Nishimura, Y., 1995, *J. chem. Phys.*, **103,** 3895.
[29] Ozeki, H., Takaahashi, M., Okuyama, K., and Kimura, K., 1993, *J. chem. Phys.*, **99,** 56.
[30] Tanaka, K., Honjyo, H., Tanaka, T., Takaguchi, H., Ohshima, Y., and Endo, Y., 1991, *Abstracts of the Meeting on Molecular Structure*, Yokohama, Japan, p. 223.
[31] Mitsuzuka, A., Fujii, A., Ebata, T., and Mikami, N., 1996, *J. chem. Phys.*, **105,** 2618.
[32] Frost, R. K., Hagemeister, F. C., Arrington, C. A., and Zwier, T. S., 1996, *J. chem. Phys.*, **105,** 2595; Frost, R. K., Hagemeister, F. C., Arrington, C. A., Schleppenbach, D., Zwier, T. S., and Jordan, K. D., 1996, *J. chem. Phys.*, **105,** 2605.
[33] Sheringer, C., Wehehahn, O. J., and Stackelberg, M. V., 1906, *Z. Electrochem.*, **64,** 381,
[34] Groth, P., 1971, *Chem. Cristallogr.*, **4,** 72.
[35] Fuke, K., and Kaya, K., 1982, *Chem. Phys. Lett.*, **91,** 311; Fuke, K., and Kaya, K., 1983, *Chem. Phys. Lett.*, **94,** 97.
[36] Connel, L. L., Ohline, S. M., Joireman, P. W., Corcoran, T. C., and Felker, P. M., 1992, *J. chem. Phys.*, **96,** 2585.
[37] Ebata, T., Watanabe, T., and Mikami, N., 1995, *J. chem. Phys.*, **99,** 5761.
[38] Brutschy, B., Janes, C., and Eggert, J., 1988, *Ber. Bunsenges. Physik. Chem.*, **92,** 435; Brutschy, B., 1990, *J. phys. Chem.*, **94,** 8637; Brutschy, B., Eggert, J., Janes, C., and Baumgärtel, H., 1991, *J. phys. Chem.*, **95,** 5041.
[39] Fujii, A., Okuyama, S., Iwasaki, A., Maeyama, T., Ebata, T., and Mikami, N., 1996, *Chem. Phys. Lett.*, **256,** 1.
[40] Maeyama, T., and Mikami, N., 1988, *J. Am. chem. Soc.*, **110,** 7238; Maeyama, T., and Mikami, N., 1990, *J. phys. Chem.*, **94,** 6973.
[41] Djafari, S., Barth, H. D., Buchhol, D. K., and Brutschy, B. J., 1997, *J. chem. Phys.*, **107**, 10573.
[42] Schwarz, H. A., 1977, *J. chem. Phys.*, **67,** 5525.
[43] Price, J. M., Crofton, M. W., and Lee, Y. T., 1989, *J. chem. Phys.*, **91,** 2749; Price, J. M., Crofton, M. W., and Lee, Y. T., 1991, *J. phys. Chem.*, **95,** 2182.
[44] Wang, Y. S., Jiang, J. C., Cheng, C. L., Lin, S. H., Lee, Y. T., and Chang, H. C., 1997, *J. chem. Phys.*, **107**, 9695.
[45] Liu, W. L., and Lisy, J. M., 1988, *J. chem. Phys.*, **89,** 605; Draves, J. A., Luthey-Schulten, Z., Liu, W. L., and Lisy, J. M., 1990, *J. chem. Phys.*, **93,** 4589; Selegue, T. J., Moe, N., Draves, J. A., Lisy, J. M., 1992, *J. chem. Phys.*, **96,** 7268; Selegue, T. J., and Lisy, J. M., 1992, *J. phys. Chem.*, **96,** 4143.
[46] Selegue, T. J., Cabarcos, O. M., and Lisy, J. M., 1994, *J. chem. Phys.*, **100,** 4790; Weinheimer, C. J., and Lisy, J. M., 1996, *J. chem. Phys.*, **105,** 2938; Weinheimer, C. J.,

and LISY, J. M., 1996, *J. phys. Chem.*, **100,** 15305; WEINHEIMER , C. J., and LISY, J. M., 1996, *Int. J. Mass. Spectrometry Ion Processes*, **159,** 197.

[47] ICHIHASHI , M., YAMABE, J., MURAI, K., NONOSE, S., HIRAO, K., and KONDO , T., 1996, *J. phys. Chem.*, **100,** 10050.

[48] CAO, Y., CHOI, J. H., HAAS, B. M., JOHNSON , M. S., and OKUMURA , M., 1993, *J. chem. Phys.*, **99,** 9307; CHOI, J. H., KUWATA , K. T., HAAS, B. M., JOHNSON , M. S., OKUMURA , M., 1994, *J. chem. Phys.*, **100,** 7153; CAO, Y., CHOI, J. H., HAAS, B. M., and OKUMURA , M., 1994, *J. phys. Chem.*, **98,** 12176.

[49] NAKANAGA , T., SUGAWARA , K., KAWAMATA , K., and ITO, F., 1997, *Chem. Phys. Lett.*, **267,** 491.

[50] MEUWLY , M., NIZKORODOV , S. A., MAIER, J. P., and BIESKE, E. J., 1996, *J. chem. Phys.*, **104,** 1996.

[51] SAWAMURA , T., FUJII, A., SATO, S., EBATA, T., and MIKAMI , N., 1996, *J. phys. Chem.*, **100,** 8131.

[52] FUJII, A., IWASAKI , A., YOSHIDA , K., EBATA, T., and MIKAMI , N., 1997, *J. phys. Chem.*, **A101,** 1798.

[53] SATO, S., EBATA, T., and MIKAMI , N., 1994, *Spectrochimica Acta*, **50A,** 1413.

[54] OHASHI , K., and NISHI , N., 1992, *J. phys. Chem.*, **96,** 2931; NAKAI, Y., OHASHI , K., and NISHI , N., 1992, *J. phys. Chem.*, **96,** 7873.

[55] CHESHNOVSKY , O., and LEUTWYLER , S., 1988, *J. chem. Phys.*, **88,** 4127.

[56] SATO, S., and MIKAMI , N., 1996, *J. phys. Chem.*, **100,** 4075.

[57] BEGEMANN , M. H., and SAYKALLY , R. J., 1985, *J. chem. Phys.*, **82,** 3570.

[58] BOGEY , M., BOLVIN , H., DEMYUNK , C., and DESTOMBES , J. L., 1987, *Phys. Rev. Lett.*, **58,** 988.

[59] OKUMURA , M., YEH, L. I., MYERS, J. D., and LEE, Y. T., 1989, *J. phys. Chem.*, **94,** 3416.

[60] BOO, D. W. and LEE, Y. T., 1995, *J. chem. Phys.* **103,** 520; BOO, D. W. and LEE, Y. T., 1996, *Int. J.Mass Spectrometry Ion Processes*, **159,** 209.

[61] FUJII, A., SAWAMURA , T., TANABE , S., EBATA, T., and MIKAMI , N., 1994, *Chem. Phys. Lett.*, **225,** 104.

[62] FUJII, A., IWASAKI , A., EBATA, T., and MIKAMI , N., 1997, *J. phys. Chem.*, **A101,** 5963; FUJII, A., IWASAKI , A., and MIKAMI , N., 1997, *Chem. Lett.*, 1099.

[63] MÜLLER -DETHLEFS , K., and SCHLAG , E., 1991, *Ann. Rev. phys. Chem.*, **42,** 109.

[64] TAYLER , D. P., GOODE, J. G., LECLAIRE , J. E., and JOHNSON , P. M., 1995, *J. chem. Phys.*, **103,** 6293; GOODE, J. G., LECLAIRE , J. E., and JOHNSON , P. M., 1996, *Int. J. Mass Spectrometry Ion Processes*, **159,** 49.